Published in final edited form as:
Sci Signal. ; 2(75): ra28. doi:10.1126/scisignal.2000202.

Suppression of LPS-Induced TNF-α Production in Macrophages by cAMP Is Mediated by PKA-AKAP95-p105

Estelle A. Wall[1,*,†], **Joelle R. Zavzavadjian**[1,*,‡], **Mi Sook Chang**[1,*,§], **Baljinder Randhawa**[1,‖], **Xiaocui Zhu**[1,¶], **Robert C. Hsueh**[2,#], **Jamie Liu**[1], **Adrienne Driver**[1,**], **Xiaoyan Robert Bao**[1,††], **Paul C. Sternweis**[2], **Melvin I. Simon**[1,†], and **Iain D. C. Fraser**[1,‡‡,§§]

[1]Alliance for Cellular Signaling, Division of Biology, California Institute of Technology, Pasadena, CA 91125, USA

[2]Alliance for Cellular Signaling, Department of Pharmacology, University of Texas Southwestern Medical Center, Dallas, TX 75390, USA

Abstract

The activation of macrophages through Toll-like receptor (TLR) pathways leads to the production of a broad array of cytokines and mediators that coordinate the immune response. The inflammatory potential of this response can be reduced by compounds, such as prostaglandin E_2, that induce the production of cyclic adenosine monophosphate (cAMP). Through experiments with cAMP analogs and multigene RNA interference (RNAi), we showed that key anti-inflammatory effects of cAMP were mediated specifically by cAMP-dependent protein kinase (PKA). Selective inhibitors of PKA anchoring, time-lapse microscopy, and RNAi screening suggested that differential mechanisms of PKA action existed. We showed a specific role for A kinase-anchoring protein 95 in suppressing the expression of the gene encoding tumor necrosis factor-α, which involved phosphorylation of p105 (also known as Nfkb1) by PKA at a site adjacent to the region targeted by inhibitor of nuclear factor κB kinases. These data suggest that crosstalk between the TLR4 and cAMP pathways in macrophages can be coordinated through PKA-dependent scaffolds that localize specific pools of the kinase to distinct substrates.

INTRODUCTION

The activation of Toll-like receptors (TLRs) triggers a complex cellular response that activates multiple intracellular signaling pathways (1–3). Control of the activation of these pathways in monocyte-derived cells is critical; excessive activation can lead to chronic inflammatory disorders, whereas insufficient activation can render the host susceptible to infection. In the case of the TLR pathways, several mechanisms of feedback control have been identified involving negative regulators that are induced by activation of TLRs (4–7). Bacterial pathogens have also developed mechanisms to evade the host response through the inhibition of signaling

§§To whom correspondence should be addressed. fraseri@niaid.nih.gov.
*These authors contributed equally to this work
†Present address: Department of Pharmacology, University of California, San Diego, La Jolla, CA 92093, USA.
‡Present address: TMT Observatory Corporation, Pasadena, CA 91125, USA.
§Present address: Children's Hospital Los Angeles, Los Angeles, CA 90027, USA.
‖Present address: Xencor, Monrovia, CA 91016, USA.
¶Present address: Astellas Research Institute of America, Skokie, IL 60077, USA.
#Present address: Cadent Medical Communications, Irving, TX 75063, USA.
**Present address: Truman College, Chicago, IL 60640, USA.
††Present address: Massachusetts General Hospital, Boston, MA 02114, USA.
‡‡Present address: Program in Systems Immunology and Infectious Disease Modeling, National Institute of Allergy and Infectious Diseases, National Institutes of Health, Bldg. 33, Rm. 3W20B.4, 33 North Drive, MSC-8180, Bethesda, MD 20892, USA.

by mitogen-activated protein kinase (MAPK) and nuclear factor κB(NF-κB) proteins (8,9), which constitute two of the major signaling pathways activated by TLRs.

Macrophages represent one of the key cell types in the innate immune system. To further understand the strategies that these cells use to modulate the innate immune response, we focused on the effects of the induction of cyclic adenosine monophosphate (cAMP) production on the processes mediated by TLR activation. In previous work, we showed that all combinations of TLR ligands [lipopolysaccharide (LPS), PAM_2CSK (P2C), PAM_3CSK (P3C), and resiquimod-848 (R848)] when added to macrophages with ligands that induced the production of cAMP [isopreternol (ISO) and prostaglandin E_2 (PGE_2)] showed nonadditive outputs in the secretion of select cytokines, which suggests the existence of conserved mechanisms of crosstalk between these pathways (10,11). The production of TLR-dependent proinflammatory cytokines such as tumor necrosis factor-α (TNF-α) and macrophage inflammatory protein 1α (MIP-1α) is substantially suppressed in the presence of PGE_2 or ISO, whereas the secretion of cytokines associated with anti-inflammatory activity in macrophages, such as interleukin-10 (IL-10) and granulocyte colony-stimulating factor (G-CSF), is markedly increased in the presence of PGE_2 or ISO. It is well established that cAMP elicits an anti-inflammatory effect on the immune system (12), but the cellular and molecular mechanisms underlying these effects in monocyte-derived cells have not been clearly elucidated (13–22). We chose to study the interactions between these signaling pathways to gain insight into the mechanisms used by the cell to modulate the TLR response in a context-dependent manner.

Here, we showed that the effects of cAMP on LPS-induced cytokine secretion in the RAW 264.7 macrophage cell line were dependent on cAMP-dependent protein kinase (PKA) and that most of these effects also required specific localization of the kinase through A kinase-anchoring proteins (AKAPs). Moreover, differential effects of cAMP on the production of pro- and anti-inflammatory cytokines were mediated by different classes of AKAP-PKA complexes. Specific investigation of cAMP-dependent suppression of LPS-induced expression of *TNF*-α uncovered a pathway through which AKAP95-targeted PKA modulated the NF-κB pathway through phosphorylation of p105 (also known as Nfkb1).

RESULTS

Proximal mediators of the effects of PGE_2 on LPS-induced expression of cytokine genes in RAW 264.7 cells

To determine whether the observed effects of cAMP on LPS-induced secretion of cytokines in RAW 264.7 cells (10,11) were observed at the level of gene transcription, we carried out real-time, reverse transcription polymerase chain reaction (RT-PCR) analysis of the abundance of TNF-α, MIP-1α, IL-10, and G-CSF messenger RNAs (mRNAs) in RAW cells stimulated with LPS, PGE_2, or both ligands. The suppressive effect of PGE_2 on LPS-induced secretion of TNF-α and MIP-1α secretion was also observed at the level of transcription (Fig. 1, A and B). Similarly, the enhancement of LPS-induced secretion of IL-10 and G-CSF in the presence of PGE_2 was also reflected in the abundance of their mRNAs (Fig. 1, C and D). These results showed that the crosstalk between LPS-stimulated and PGE_2-stimulated signaling pathways occurred either upstream of, or at the level of transcription.

Because PGE_2 activates members of a receptor family (EP1 to EP4) that signal through a range of heterotrimeric guanine nucleotide-binding protein (G protein) families to stimulate either cAMP or Ca^{2+} signals (23), we wanted to confirm that the effects of PGE_2 on cytokine production were mediated by cAMP. In experiments with the cell-permeable cAMP analog 8Br-cAMP, we observed a robust suppression of LPS-induced expression of *TNF*-α and *MIP*-1α and an enhancement in LPS-induced expression of *IL-10* and *G-CSF* (Fig. 1, E and F).

The primary mediator of the cellular response to cAMP is the cAMP-dependent protein kinase (PKA) (24); however, studies have identified another important cellular target of cAMP, the guanine nucleotide exchange factor known as exchange protein activated by cAMP (EPAC) (25). Assessment of PKA and EPAC isoforms by microarray analysis and quantitative PCR (qPCR) assays suggested that mRNA transcripts of PKA-RIα, PKA-RIIα, PKA-RIIβ, PKA-Cα, PKA-Cβ, EPAC1, and EPAC2 were found in RAW 264.7 cells (fig. S1). Other studies of macrophages have suggested that the cAMP-dependent suppression of LPS-induced production of TNF-α is mediated by PKA, whereas the inhibition of phagocytic activity by cAMP is mediated by EPAC (13,20,22). The implication that PKA controls the production of TNF-α has generally been based on use of the chemical inhibitor of PKA, H-89; however, we have found that the use of H-89 in RAW cells to inhibit PKA activity gives inconsistent results, with incomplete reversal of cAMP-mediated suppression of LPS-induced production of TNF-α (10).

Here, we used two approaches to address which target of cAMP was responsible for the modulation of LPS-induced expression of cytokine genes. First, we used analogs of cAMP that were developed to be selective for PKA and EPAC (26), and we determined their effect on LPS-induced production of TNF-α and MIP-1α. Suppression of LPS-induced secretion of TNF-α or MIP-1α (Fig. 1G) or enhancement of LPS-induced secretion of IL-10 or G-CSF (Fig. 1H) was achieved with the PKA-selective analog 6Bz-cAMP. On the other hand, the EPAC-selective analog 8pCPT-2′OMe-cAMP had minimal effects on the LPS-induced secretion of these cytokines. These data suggest that both the cAMP-mediated suppression of LPS-induced production of TNF-α and MIP-1α and the enhancement of LPS-induced production of IL-10 and G-CSF were primarily mediated by PKA.

To test this hypothesis more directly, we performed additional experiments to knockdown PKA through RNA interference (RNAi) technology. Because both the α and the β isoforms of the PKA catalytic subunit are found in RAW cells, we took advantage of our previously described vector platform for multigene RNAi (27). Because RAW cells are intractable to high-efficiency transfection with short interfering RNA (siRNA), we developed retroviral vectors that enabled the expression of multiple microRNA (miR)-based short hairpin RNAs (shRNAs) from a single transcript (Fig. 2A). Because the miR-shRNAs are designed as mimics of miRNAs (28), they are processed into gene-specific siRNAs by the endogenous miRNA-processing machinery of the cell. This approach enabled us to create stably transfected RAW cell lines depleted of PKA-Cα,PKA-Cβ, or both isoforms (Fig. 2B).

To determine whether these cells displayed compromised PKA signaling, we assessed the phosphorylation status of a known substrate of PKA, the vasodilator-stimulated phosphoprotein (VASP) (29), in response to an increase in cAMP concentration. We saw no reduction in the abundance of phosphorylated VASP in response to 8Br-cAMP when either PKA-Cα or PKA-Cβ subunit was depleted, which suggested that the subunits were functionally redundant with respect to phosphorylation of VASP (Fig. 2C). However, we saw a substantial reduction (>86%) in 8Br-cAMP-dependent phosphorylation of VASP when both PKA-C subunits were depleted (Fig. 2C). To assess the effect of knockdown of PKA on crosstalk between the TLR and cAMP pathways, we used these miR-shRNA-expressing cell lines to analyze the abundance of cytokine mRNAs in response to stimulation by the appropriate ligands. Once again, we found that knockdown of either PKA catalytic subunit had no effect on cAMP-dependent suppression of LPS-induced expression of *TNF*-α or *MIP-1*α or on LPS-induced enhancement of the expression of *IL-10* or *G-CSF* (Fig. 2, D to G). Remarkably, the effects of cAMP on LPS-induced expression of cytokine genes were almost completely reversed in the PKA-Cα and PKA-Cβ double knockdown cell line (Fig. 2, D to G). These data provided strong evidence that the anti-inflammatory effect of cAMP on the production of cytokines from macrophages was mediated by PKA. Knockdown of both PKA-C subunits had

no substantial effect on LPS-induced expression of *MIP-1α*, *IL-10*, or *G-CSF* (Fig. 2, E to G). The fold induction in the abundance of TNF-α mRNA by LPS (from an equivalent basal abundance of TNF-α mRNA in each cell line) was greater in the double knockdown cell line (29.71 ± 8.05) than in the control cell line (7.91 ± 0.89). This suggests that PKA has a role in attenuating the expression of *TNF*-α after stimulation of macrophages by LPS.

Distinct PKA-dependent mechanisms for modulation of LPS-induced cytokines

It is well known that many of the cellular effects of PKA are controlled by localization of the kinase to specific cellular compartments. This is achieved by the specific interaction of the regulatory subunits of PKA with AKAPs, which position the kinase in close proximity to its substrate(s) (30,31). To determine whether the PKA-dependent modulation of LPS-induced activation of macrophages required anchoring of the kinase, we used peptides designed to disrupt interactions between AKAPs and PKA. The prototypical PKA-anchoring inhibitor peptide, Ht31, primarily disrupts interactions between AKAPs and the type II PKA holoenzyme through its nanomolar affinity for the type II regulatory subunit (RII) (Fig. 3A) (32). It has also been established that certain AKAPs can also bind to the type I PKA holoenzyme (33), and this has led to the development of an anchoring inhibitor peptide, RIAD, which binds with nanomolar affinity to the PKA type I regulatory subunit (RI) (Fig. 3A) (34). To confirm the specificity of these reagents in RAW 264.7 cells, we preincubated cells with the anchoring inhibitor peptides or with the corresponding control peptides and assessed their ability to deplete RI or RII from the particulate fraction of RAW cells (fig. S2). These experiments confirmed that 100 μM Ht31 and 50 μM RIAD mediated specific disruption of the partitioning of the RII (fig. S2A) and RI (fig. S2B) subunits of PKA, respectively.

We then proceeded to determine how these peptides affected the ability of PGE_2 to modulate LPS-induced expression of cytokine genes. The Ht31 peptide reversed the PGE_2-dependent attenuation of the LPS-induced expression of *TNF*-α and *MIP-1α*, but had no effect on PGE_2-dependent enhancement of LPS-induced expression of *IL-10* and *G-CSF* (Fig.3, B to E). In contrast, the RIAD peptide had no effect on the ability of PGE_2 to suppress LPS-induced expression of *TNF*-α and *MIP-1α* or to enhance LPS-induced expression of *IL-10*, but it reduced the PGE_2-dependent enhancement of LPS-induced expression of *G-CSF*. This shows not only that many of the effects of PKA on the activation of macrophages are dependent on localization of the kinase, but also that the nature of the PKA-AKAP complex may explain how the kinase can promote opposing modulatory effects on LPS-induced expression of cytokine genes. A single cAMP-inducing stimulus, in this case PGE_2, promoted suppression of LPS-induced expression of *TNF*-α and *MIP-1α* through a process that required anchoring of type II PKA (Fig. 3, B and C) while simultaneously enhancing LPS-induced expression of *G-CSF* through a process that required type I anchored PKA (Fig. 3E). Moreover, the data suggest that the enhancement of LPS-induced expression of *IL-10* occurred through yet another process that, although PKA dependent (Fig. 2F), did not appear to require anchoring of the kinase (Fig. 3D).

It has been proposed that the molecular basis for cAMP-dependent suppression of the LPS-induced expression of *TNF*-α involves competition for transcriptional cofactors by the transcription factor cAMP response element-binding protein (CREB). A mechanism was proposed whereby activated CREB competes directly with NF-κB for common cofactors, such as CREB-binding protein (CBP)/p300, which leads to reduced NF-κB-mediated transcription of *TNF*-α (14,16). To address whether this mechanism contributed to the cAMP-dependent suppression of LPS-induced expression of *TNF*-α in RAW cells, we generated a RAW cell line stably expressing a CREB1a-specific shRNA with the same retroviral approach described earlier. We were able to achieve consistent knockdown of about 80% of CREB1a in this cell line (fig. S3). We then compared the cAMP-dependent modulation of the expression of cytokine genes in this cell line (shCreb) to that of a control line expressing a shRNA against

luciferase (shLuc). We saw no difference in the cAMP-dependent modulation of the expression of *TNF*-α, *MIP-1*α,or *G-CSF* in these cell lines (Fig. 3, F, G, and I), which suggests that competition for transcriptional cofactors was not a major contributory factor to the effects of cAMP in these cells. We did observe, however, almost complete loss of the cAMP-dependent enhancement of LPS-induced *IL-10* expression in the shCreb cell line (Fig. 3H). This suggested a mechanism whereby the modulatory effects of PKA that required anchoring of the kinase (suppression of *TNF*-α and *MIP1*-α expression and enhancement of *G-CSF* expression) were independent of the activation of CREB, whereas the anchoring-independent enhancement of *IL-10* expression was dependent on CREB.

Evaluation of the NF-κB pathway as a target for PKA-dependent modulation of macrophage activation

LPS-induced activation of macrophages leads to stimulation of the transcription of cytokine genes through both MAPK and NF-κB pathways (1,2). We speculated that because much of the crosstalk between the PKA and TLR4 pathways appeared to be independent of CREB, PKA might directly influence the degree of activation of the MAPK or NF-κB pathways by LPS. In experiments with phosphospecific antibodies specific for multiple MAPKs, including p38 MAPK, c-Jun N-terminal kinase (JNK), and extracellular signal-regulated kinase (ERK), we observed robust increases in phosphorylation in response to LPS; however, PGE_2 had no effect on the degree of activation of any of these MAPKs (fig. S4).

We next assessed activation of the canonical NF-κB pathway by measuring the LPS-induced degradation of inhibitor of NF-κB (IκBα) in RAW cells and primary bone marrow-derived macrophages (BMDMs). We observed the characteristic degradation of IκBα followed by recovery of the protein in response to LPS (35), but we did not see any substantial effect of either 8Br-cAMP or PGE_2 on this process (Fig. 4, A and B). We also considered the phosphorylation status of NF-κB p65 (also known as RelA) as an indicator of activation of the NF-κB pathway, and, because p65 is proposed to be a substrate of PKA (36), phosphorylation of p65 is also a candidate mechanism through which PKA could mediate its modulatory effect on the expression of cytokine genes. We initially assessed phosphorylation at Ser^{536} in the C-terminal transactivation domain of p65, because this is the primary phosphorylation site for the IκB kinase (IKK) family and leads to enhanced transactivation potential (37). Activation of RAW cells with LPS induced a fourfold increase in the abundance of p65 phosphorylated at Ser^{536} compared to that in untreated cells, but we did not observe any change in this extent of phosphorylation in the presence of 8Br-cAMP (fig. S5).

It has been proposed that the catalytic subunit of PKA has an unusual role in the LPS-induced activation of NF-κB through its cAMP-independent phosphorylation of p65 at Ser^{276}. Ghosh and colleagues proposed that the catalytic subunit of PKA interacts directly with IkBa and that LPS-induced degradation of IκBα releases the kinase to phosphorylate Ser^{276} of p65 and promote its transactivation potential through the enhanced recruitment of histone acetyltransferases (36,38). To determine if this mechanism for phosphorylation of p65 is prevalent in RAW cells, we assessed the LPS-induced phosphorylation of p65 at Ser^{276} in our cell lines depleted of PKA-Cα and PKA-Cβ, but we saw little effect on the phosphorylation at this site, even in cells lacking both catalytic subunits of PKA (Fig. 4C). This site is also an excellent substrate for mitogen- and stress-activated protein kinase 1 (MSK1) (39), which is activated in macrophages by LPS (40). This suggests that in our studies, MSK1 is the more likely mediator of the LPS-induced phosphorylation of p65 at Ser^{276}, and that the cAMP-independent phosphorylation of this site by PKA through the mechanism described by Ghosh and colleagues is not likely to be a substantial factor in our experiments. However, this site was phosphorylated by PKA in a cAMP-dependent manner in RAW cells, because 8Br-cAMP increased the abundance of p65 protein phosphorylated at Ser^{276}, albeit to a lower extent than

that promoted by LPS-induced activation of MSK1 (Fig. 4D). Furthermore, because the combination of LPS and 8Br-cAMP did not appear to enhance the abundance of p65 protein phosphorylated at Ser^{276} (Fig. 4D), it seems unlikely that phosphorylation of p65 at this site is a key point of crosstalk between the TLR4 and cAMP pathways in macrophages.

We used electrophoretic mobility shift assay (EMSA) experiments to assess the nuclear accumulation of NF-κB complexes in RAW cells stimulated with LPS for up to 4 hours. We saw robust nuclear accumulation of the canonical NF-κB p50–p65 heterodimer after 30 min of treatment, with gradual loss of the nuclear complex by 4 hours (Fig. 4E). Identification of both p50–p65 and the p50–p50 homodimer in the EMSA studies was confirmed by supershift analysis (Fig. 4, F and G). Costimulation of cells with LPS and 8Br-cAMP slowed the nuclear accumulation of p50–p65 compared to that in LPS-treated cells (Fig. 4E), which could conceivably account for the attenuated expression of proinflammatory, early response genes such as *TNF*-α and *MIP-1α*. In addition, 8Br-cAMP increased the nuclear accumulation of p50–p50 after 4 hours of stimulation compared to that in LPS-stimulated cells (Fig. 4E). Because the p50–p50 homodimer inhibits transcription from promoters that contain NF-κB sites (35), this effect of cAMP could contribute to the suppression of LPS-induced expression of NF-κB-dependent genes. The increased abundance of p50–p50 in the presence of 8Br-cAMP is consistent with a report that the binding of p50 to DNA is promoted by its phosphorylation by PKA (41).

In a parallel experimental approach, we generated a RAW cell line stably expressing a green fluorescent protein (GFP)-tagged fusion of the NF-κB p65 protein, which permitted assessment of NF-κB activation by monitoring the translocation of GFP-p65 from the cytosol to the nucleus (42). Activation of these cells by LPS stimulated the nuclear translocation of GFP-p65, as measured by time-lapse confocal microscopy (Fig. 5, A to D). When these cells were stimulated with both LPS and 8Br-cAMP, translocation of GFP-p65 was still observed, but the kinetics of the process were delayed compared to that in cells treated with LPS alone (Fig. 5, E to H). Data averaged from multiple cells suggested an approximate 20-min delay in the nuclear translocation of GFP-p65 in the presence of cAMP (Fig. 5I). To determine if this attenuation of translocation of GFP-p65 by cAMP was dependent on the anchoring of PKA, we repeated the experiments in the presence of the Ht31 and RIAD peptides. The RIAD peptide had no substantial effect on the attenuation of translocation of p65 by cAMP; however, the Ht31 peptide ablated the inhibitory effect of cAMP on nuclear translocation of GFP-p65 (Fig. 5J). These results further support the hypothesis that the attenuation of LPS-induced translocation of p65 by cAMP underlies the inhibitory effect of cAMP on the expression of genes encoding proinflammatory cytokines (TNF-α and MIP-1α), because these effects were also selectively reversed by Ht31 (Fig. 3, B and C). The lack of an effect with the RIAD peptide further indicates that type I PKA anchoring-dependent enhancement of LPS-induced expression of *G-CSF* did not depend on the attenuation of p65 translocation.

Identification of potential mediators of cAMP-TLR crosstalk upstream of the expression of *TNF*-α

The effects observed with the Ht31 peptide suggested that a type II PKA-AKAP interaction might underlie the attenuation of LPS-induced expression of *TNF*-α by cAMP. To investigate this further, we used RNAi to target AKAPs found in RAW cells. A combination of microarray analysis, qPCR assays, and Western blot-based PKA binding analysis suggested that a group of 10 AKAP proteins were detectable in RAW cells (fig. S6). We used RNAi to deplete these proteins in RAW cells before assessing PGE_2-dependent attenuation of LPS-induced expression of *TNF*-α. We found that the inhibition of LPS-induced expression of *TNF*-α by PGE_2 was lost in RAW cells depleted of AKAP95 (also known as AKAP8) (Fig. 6A) but was not substantially affected by knockdown of any of the other nine AKAP proteins.

We previously generated a library from macrophage mRNA and identified several candidate binding partners for AKAP95 through yeast two-hybrid experiments (http://www.signaling-gateway.org/data/Y2H/cgi-bin/y2h_int.cgi?id=18288). Several proteins identified in this screen suggested a potential role for AKAP95 in the modulation of macrophage activation pathways. We were particularly interested in the identification of a component of the NF-κB family, p105 (also known as Nfkb1), which represents both the precursor protein for p50 and, in the full-length p105 polypeptide, a protein with potential IκB function(43). A schematic of the domain structure of both AKAP95 and p105 highlights the regions of potential interaction on the basis of the protein fragments that interact in yeast (Fig. 6B). AKAP95 has been primarily characterized as a nuclear protein (44), so it is noteworthy that the nuclear membrane-targeting sequence (NMTS) and the nuclear location signal (NLS) are contained within the region proposed to interact with p105. Western blotting analysis of cytosolic and nuclear fractions from RAW cells showed that although most of AKAP95 was found in the nucleus, some AKAP95 was cytosolic (Fig. 6C). Because p105 was exclusively cytosolic (Fig. 6C), it is possible that an interaction with p105 retained a pool of AKAP95 in the cytoplasm of RAW cells, possibly through the masking of the nuclear-targeting sequences of AKAP95. To determine whether AKAP95 and p105 were present in a complex in mammalian cells, FLAG-tagged AKAP95 was coexpressed with Myc-tagged p105 in human embryonic kidney (HEK) 293 cells. Immunoprecipitation of either protein pulled down a complex containing AKAP95, p105, and PKA-Cα (Fig. 6D). To assess whether endogenous p105 and AKAP95 associated with each other in macrophages, both RAW cells and primary BMDMs were fractionated into cytosolic and nuclear fractions, which were subjected to immunoprecipitation with p105-specific antisera. In both cell types, AKAP95 coimmunoprecipitated with p105 specifically from the cytosolic fraction (Fig. 6E).

Requirement for AKAP95-mediated anchoring of PKA for cAMP-dependent suppression of *TNF*-α expression in primary macrophages

To assess the role that AKAP95-mediated targeting of PKA might play in the effects of cAMP on primary macrophages, we isolated BMDMs from mice expressing a gene-trapped mutant of AKAP95 that does not bind to PKA (45) ($AKAP95^{GT}$). In BMDMs from wild-type (WT) mice, PGE_2 attenuated the LPS-induced expression of *TNF*-α (Fig. 7A), and the PGE_2 dose-response profile suggested that this attenuation was observed at the nanomolar concentrations of PGE_2 predicted to be present in vivo (46) (Fig. 7B). To determine whether AKAP95-targeted PKA might be involved in this process, we compared the effect of PGE_2 on LPS-induced expression of *TNF*-α in BMDMs derived from WT mice and $AKAP95^{GT}$ mice (Fig. 7, C and D). We found that PGE_2-mediated attenuation of LPS-induced expression of *TNF*-α by PGE_2 in $AKAP95^{GT}$ mice was not observed after 30 or 60 min of treatment, but was comparable to that of WT cells at later time points. These results support a mechanism whereby AKAP95-targeted PKA is required for the cAMP-dependent attenuation of the expression of *TNF*-α in the early stages after exposure to LPS.

Functional implications of PKA-mediated phosphorylation of p105

Signals that promote the activation of NF-κB in macrophages lead to phosphorylation of IκB family proteins by the IKK family (47). Accordingly, p105 is phosphorylated by IKKs on numerous Ser residues near its C terminus, which triggers its degradation through a proteasome-dependent pathway (48,49). We noticed that murine p105 contains a consensus PKA phosphorylation site ($RKLS^{940}F$) adjacent to its IKK target sites, and that this sequence is conserved in other mammalian p105 paralogs. To assess whether this sequence could be phosphorylated by PKA, we expressed and purified the sequence as a glutathione *S*-transferase (GST) fusion protein, which we used for in vitro kinase assays. We used the sequence around Ser^{157} in the VASP protein as a positive control and showed that this sequence was phosphorylated by PKA in vitro, whereas a sequence in which Ser^{157} was mutated to Ala was

not (Fig. 8A). Ser^{940} of p105 was phosphorylated by PKA to a similar extent, whereas no phosphorylation of the same sequence occurred when Ser^{940} was substituted by Ala (Fig. 8B).

We assessed whether p105 could be phosphorylated by PKA in intact cells by immunoprecipitating p105 from RAW 264.7 cells in which PKA activity had been increased by treatment with either calyculin A or a combination of calyculin A and 8Br-cAMP. In experiments with a phosphospecific antibody raised against a consensus PKA sequence, we observed the appearance of a phosphoprotein of 105 kD after activation of PKA (Fig. 8C). PGE_2 suppresses LPS-induced degradation of p105 (50). To determine whether phosphorylation of p105 at Ser^{940} by PKA might underlie this effect of PGE_2, we assessed the effect of cAMP on LPS-induced degradation of WT p105 and mutant p105 proteins in which Ser^{940} was mutated to either Ala or Asp residues. In accordance with previous observations, the LPS-induced reduction in the abundance of p105 protein was blocked by cAMP (Fig. 8D, top). In contrast, LPS-induced degradation of the Ser^{940}→Ala mutant p105 protein (which cannot be phosphorylated by PKA) was unaffected by cAMP (Fig. 8D, middle), whereas there was little effect of LPS on the abundance of the Ser^{940}→Asp phosphomimetic mutant p105 protein (Fig. 8D, bottom).

We speculated that cAMP-induced phosphorylation of p105 at Ser^{940} might influence the LPS-induced, IKK-mediated phosphorylation of murine p105 at an adjacent Ser residue, Ser^{935}, which is a prerequisite for degradation of p105 (48,49). LPS induced the phosphorylation of p105 at Ser^{935} in WT BMDMs, and this was attenuated by PGE_2, especially at 20 and 30 min (Fig. 8, E and G). In contrast, attenuation of LPS-induced phosphorylation of p105 at Ser^{935} by PGE_2 was lost in BMDMs from $AKAP95^{GT}$ mice (Fig. 8, F and H). These data imply that p105 could be a key substrate for PKA in the cAMP-dependent attenuation of LPS-induced expression of *TNF*-α. Mechanistically, phosphorylation of p105 at Ser^{940} by PKA appeared to attenuate the extent of IKK-dependent phosphorylation of p105 at Ser^{935}, which could in turn influence the rate of activation of NF-κB.

DISCUSSION

In this report, we investigated the mechanisms underlying crosstalk between the TLR4 and cAMP pathways in macrophages. The suppressive effect of cAMP on the activation of immune cells has been known for many years (12). In monocyte-derived cells, cAMP attenuates LPS-induced production of proinflammatory cytokines such as TNF-α (13,15,16,18,20,22) and MIP-1α (17), whereas it enhances the production of mediators with more anti-inflammatory effects on macrophages, such as IL-10 (51) and G-CSF (52–54). Some studies have used analogs of cAMP to address the relative contributions of the most likely cAMP effectors: PKA and EPAC, to inhibiting the production of TNF-α (20,22); however, most previous studies have used the inhibitor H-89 to implicate PKA in cAMP-mediated effects. Although potent in its inhibition of PKA, H-89 also shows strong inhibitory activities against other kinases, including MSK1, Rho-associated kinase 2 (ROCK2), S6 kinase 1, and Akt (55). Our data from experiments with selective cAMP analogs and RNAi specific for catalytic subunits of PKA showed that the effects of cAMP on LPS-induced expression of *TNF*-α, *MIP-1α*, *IL-10*, and *G-CSF* in RAW 264.7 cells were all PKA dependent; however, we found that H-89 inconsistently reversed the effects of cAMP in repeated experiments in RAW cells. This may have been caused by inhibition of some kinases (mentioned above) that can influence macrophage activation, and emphasizes that caution should be taken in interpreting results from experiments with inhibitors that can act on multiple kinases.

The ability to express miRNA-based shRNAs specific for both catalytic isoforms of PKA from a single retrovirus (27) was vital to determining the contribution of PKA to the effects of cAMP on LPS-induced expression of cytokine genes (Fig. 2). Although the reversal in the enhanced

expression of *IL-10* and *G-CSF* was incomplete in these experiments, this might have been due to incomplete knockdown of PKA and it is consistent with the observation that PKA-Cα knockout mice are viable despite the abundance of PKA-C in certain tissues of these mice being <10% of that of WT mice (56). It is also noteworthy that the fold induction in the abundance of TNF-α mRNA induced by LPS alone was higher in the PKA-C-deficient RAW 264.7 cell line than in control cells (Fig. 2D). Because the cells were stimulated for 2 hours, LPS would be expected to induce the expression of *COX-2* and the release of endogenous prostaglandins, including PGE_2. Autocrine stimulation of EP2 receptors, EP4 receptors, or both by PGE_2 could then lead to PKA-dependent attenuation of the expression of *TNF*-α (57). Accordingly, knockdown of PKA-C would limit this feedback and lead to the observed higher induction of *TNF*-α expression in the PKA-C-depleted cells compared to that in control cells. This is also consistent with the reduced abundance of LPS-induced TNF-α observed in PDE4B knockout mice (58), presumably caused by prolonged activation of PKA in the absence of LPS-induced expression of *PDE4B*. The physiological relevance of this negative feedback by prostaglandins is supported by the observation that resolution of pulmonary inflammation is compromised in COX-2 knockout mice (59).

Previous studies have suggested roles for AKAPs in various immune cell functions (34,60–62), and a report identified AKAP13 as a regulator of TLR2-induced signaling in the human monocyte cell line THP-1 (63). The use of selective PKA-anchoring inhibitor peptides enabled us to assess whether specific cellular localization of either type I or type II PKA was required for cAMP-mediated modulation of the expression of LPS-induced cytokine genes. Suppression of the expression of genes encoding proinflammatory cytokines by cAMP signaling was specifically reversed by delocalization of type II PKA, whereas the cAMP-mediated enhancement of the expression of *G-CSF* was specifically reversed by the delocalization of type I PKA. This suggests that divergent patterns of gene transcription could result from differential localization of type I and type II PKA holoenzymes, through their association with specific AKAPs (fig. S2), to substrates that activate different regulatory circuits and influence different transcriptional outcomes.

On the other hand, we showed that the PKA-dependent enhancement of LPS-induced expression of *IL-10* did not depend on localization of the kinase, but, in contrast to the other cytokine genes tested, did require the presence of CREB. CREB is activated by its phosphorylation by PKA at Ser^{133}; however, the PKA-mediated enhancement of LPS-induced expression of *IL-10* did not appear to be simply a summation of its expression induced by LPS and that induced by cAMP alone. Although expression of *IL-10* was CREB dependent, we detected negligible expression of *IL-10* in response to cAMP induced in response to PGE_2 (Fig. 1C). Thus, it appears that the effect of cAMP on *IL-10* expression was to specifically enhance expression induced by a stronger activating stimulus, such as LPS.

To address potential points of crosstalk between cAMP and the TLR4 pathway, we assessed the activation state of established intermediates in the TLR4 signaling cascade. Although previous reports from studies in THP-1 cells suggested that p38 MAPK is a potential site of crosstalk (16), we found no effect of increased cAMP concentration on the LPS-induced phosphorylation of p38, JNK, or ERK proteins in RAW 264.7 cells (fig. S4). Similarly, another point of interaction between these pathways proposed from studies in THP-1 cells, cAMP-dependent attenuation of IKK activity and the subsequent degradation of IκBα (16), was not observed in our studies (Fig. 4, A and B). This suggests that mechanisms of cAMP-mediated regulation of the TLR4 pathway may vary between different monocyte-derived cell types.

In RAW 264.7 cells, our data suggest that cAMP had specific effects on the activation dynamics of NF-κB proteins. A slowed nuclear accumulation of the p50–p65 heterodimer in the first hour after LPS stimulation was shown by both time-lapse microscopy (Fig. 5) and EMSA

experiments (Fig. 4E), whereas there was a later cAMP-dependent enhancement of p50–p50 homodimer formation after 4 hours of stimulation with LPS and an agonist of the cAMP pathway (Fig. 4E). Because the p50–p50 homodimer is proposed to be a transcriptional repressor at NF-κB-dependent promoters, both of these early and late effects of cAMP on NF-κB activity could contribute to cAMP-mediated suppression of LPS-induced expression of proinflammatory cytokine genes.

Our data on AKAP95 and p105 provide insight into the mechanistic basis of the early effect of cAMP on gene expression, which is of particular relevance to the amount of TNF-α released from activated macrophages in the early stages of infection. This is especially important in sepsis, in which high concentrations of TNF-α have serious pathological consequences (64). Our RNAi screen of the AKAPs found in RAW cells suggested that the targeting of PKA by AKAP95 was necessary for PGE_2 to mediate suppression of LPS-induced expression of *TNF*-α, and the data from experiments with BMDMs derived from $AKAP95^{GT}$ mice, which expresses a truncated AKAP95 protein that cannot bind to PKA (45), supported the hypothesis that it was the PKA-targeting function of AKAP95 that was important in this regard. It is noteworthy that only the early suppression (30 and 60 min) by PGE_2 of the expression of *TNF*-α was lost in the $AKAP95^{GT}$ mouse, whereas the suppressive effect of cAMP in BMDMs from these mice was comparable to that of BMDMs from WT mice at 2 and 4 hours (Fig. 7, C and D). It is possible that these later effects of cAMP depended on the enhanced formation of the NF-κB p50–p50 complexes observed by EMSA (Fig. 4E) and that this occurs through an additional mechanism that is independent of AKAP95.

The initial identification of p105 as a putative binding partner for AKAP95 in the Alliance for Cellular Signaling (AfCS) yeast two-hybrid screen emphasizes the value of this data resource (http://www.signaling-gateway.org/data/Y2H/cgi-bin/y2h.cgi). Moreover, the coordinates of the p105 and AKAP95 protein fragments isolated from the yeast two-hybrid screen provided additional insight to the nature of the interaction between them (Fig. 6B). Whereas AKAP95 is primarily a nuclear protein, p105 is almost exclusively cytoplasmic; however, the region of AKAP95 involved in its interaction with p105 spans the nuclear localization sequences. The presence of a cytoplasmic pool of AKAP95 in RAW 264.7 cells suggested that this may have been dependent on its interaction with p105. The identification of a similar pool of AKAP95 in Jurkat cells (65) suggests that AKAP95 may have cytoplasmic functions specific to hematopoietic lineages.

The identification of a PKA phosphorylation site in the C-terminal region of p105 suggests that p105 is a candidate substrate for AKAP95-targeted PKA. This PKA site is adjacent to several well-known IKK target sites (48,49), phosphorylation of which promote degradation of p105. Although p105 is a member of the IκB family (66), it has not been conclusively shown that it can function as a genuine IκB; that is, it has not been shown to undergo stimulus-dependent degradation to release transcription-promoting NF-κB dimers (67,68). Although we did not directly show an IκB-type function for p105 in our study, we provided evidence that the stimulus-dependent phosphorylation of p105 by IKK was inhibited by PGE_2, and that the loss of this inhibitory effect in the $AKAP95^{GT}$ mouse (Fig. 8F) was coincidental with the loss of cAMP-dependent suppression of LPS-induced, early *TNF*-α expression (Fig. 7D). This is suggestive of a mechanism whereby the earliest NF-κB complexes entering the nucleus after stimulation of macrophages by LPS have been released from inhibition by p105.

The possibility that these early complexes are not inhibited by the canonical IκB proteins is supported by the observation that PGE_2 had no effect on LPS-induced degradation of IκB in primary macrophages (Fig. 4B), despite substantially suppressing the LPS-induced expression of *TNF*-α (Fig. 7A). This mechanism is supported by a report from Libby and colleagues that identified an interaction between p105 and the EP4-associated protein, EPRAP (50). This

report also showed that PGE_2 inhibits LPS-induced phosphorylation of IKK and degradation of p105 in macrophages, and that EPRAP recruits p105 into a complex with EP4. In mice lacking EP4, the early attenuation (up to 60 min) by PGE_2 of LPS-induced expression of *TNF*-α was lost, but the later effect of PGE_2 was maintained, which is analogous to the phenotype that we observed in BMDMs from the $AKAP95^{GT}$ mouse (Fig. 7D). Together, these data suggest a mechanism whereby p105 is constitutively part of a complex with AKAP95 in the cytoplasm of macrophages and is then recruited to EP4 by EPRAP on stimulation with PGE_2. This would bring the p105-AKAP95 complex closer to the site of cAMP production, which could facilitate the activation of AKAP95-anchored PKA to phosphorylate p105 at Ser^{940}.

In summary, our results provide substantial insight into the mechanisms by which cAMP promotes its anti-inflammatory effects in macrophages. They suggest that production of this second messenger leads to a pattern of signaling that can modulate the activation of macrophages through the TLR4 pathway at multiple levels (Fig. 9). The existence of different classes of PKA-scaffolding proteins that bind selectively to different sub-types of PKA provides another layer of control to enable different modulatory effects of PKA on the cytokine profile of the activated macrophage. Our data suggest that type II PKA is targeted by AKAP95 to p105 to specifically suppress the early expression of *TNF*-α and to another component of the canonical MyD88-dependent TLR4 pathway to attenuate LPS-induced expression of *MIP-1α*. A pool of type I PKA is presumably localized to another substrate to specifically mediate enhancement of the expression of *G-CSF*. It is tempting to suggest that this enhancement might be through the MyD88-independent, TRIF-dependent component of the TLR4 pathway, because *G-CSF* has been implicated as one of the genes whose expression is induced through this pathway (69). The targeting of different pools of PKA to either arm of the TLR4 pathway would allow an increase in PKA activity to have opposite modulatory effects on different LPS-induced transcripts. We suspect that this requirement for scaffold proteins might be a recurrent theme in the analysis of signaling complexity, as scaffold proteins provide a mechanism through which the cell, armed with a limited toolbox of pleiotropic signaling effector enzymes, can organize different combinations of components to allow for context-dependent signaling (70). The anti-inflammatory mechanisms of cAMP described here may thus provide a therapeutic target for certain inflammatory disorders.

MATERIALS AND METHODS

Reagents

Reagent sources were as follows: LPS and PGE_2 (Sigma), LPS-binding protein (LBP, R&D Systems), 8Br-cAMP (Calbiochem), 8-pCPT-2′OMe-cAMP and 6Bz-cAMP (Axxora), Ht31 and Ht31c peptides (Promega), RIAD (LEQYANQLADQIIKEATE-Arg11) and scRIAD (IEKELAQQYQNADAITLE-Arg11) peptides (custom synthesized by SynBioSci Corporation, purified to >80% purity). Protocols for reagent preparation and additional procedures are provided on the AfCS Web site (http://www.signaling-gateway.org/data/ProtocolLinks.html), and are referenced by protocol number.

Cell culture and ligand treatment

RAW 264.7 cells were obtained from the ATCC and were cultured according to AfCS protocol PP00000159. BMDMs were isolated from either WT or $AKAP95^{GT}$ mice [provided by W. Frankel (45)] on the C57BL/6 background and cultured according to AfCS protocol PP00000172. Before their use in assays, RAW 264.7 cells and BMDMs were cultured for 24 hours in tissue culture-treated plates. Fresh culture medium was added to cells 1 hour before the addition of ligands, which were prepared as 10× premixes. In experiments involving Ht31

and RIAD peptides, cells were pretreated with peptides for 30 min before stimulation with ligands.

Measurement of secreted cytokines

RAW cells were cultured and stimulated as described above, and after 4 hours of incubation, the supernatants were harvested and centrifuged for 5 min at 300*g*. Aliquots were prepared and frozen until ready for cytokine measurements. G-CSF, IL-10, MIP-1α, and TNF-α were quantified with the Bio-Plex cytokine array system (Bio-Rad Laboratories, Hercules, CA) with a custom-prepared mouse cytokine assay kit for G-CSF and IL-10 and individual kits for TNF-α (Bio-Rad, 171G12221) and MIP-1α (Bio-Rad, X600004QE0).

RNA interference

Generation of miR-shRNAs targeting the PKA-Cα and PKA-Cβ subunits has been described previously (27). The miR-shRNA against murine CREB1a targeted the following sequence, 5′-GCAAGAGAATGTCGTAGAA-3′. The efficacy of the CREB1a miR-shRNA was initially tested by transient expression from the pEN_hUmiRc2 vector (71). The validated shRNA was subcloned into a retroviral expression platform by removal of the U6 promoter by digestion with Sal I and subsequent Gateway LR recombination to the pDS_FBneo vector (27). Production of retroviruses and creation of stable RAW cell lines were carried out as previously described (27). RAW cells were transiently transfected with AKAP-specific siRNAs following a previously described protocol (72). All siRNAs were siGenome SMARTpools purchased from Dharmacon.

Quantitative PCR

The abundance of mRNAs of cytokines in RAW 264.7 cells after ligand stimulation and the abundance of mRNAs targeted by RNAi were assessed by qPCR (BioRad, iCycler), following a previously described protocol (72). Sense and antisense amplification primers and probe primer sequences (where appli- cable) were as follows: TNF-a,5′-CTCAAAATTCGAGTGACAAGCCTG-3′, 5′-ATCGGCTGGCACCACTAGTT-3′,and 5′-FAM-AGCCCACGTCGTAG- CAAACCACCA-BHQ1-3′; MIP-1a,5′-CTCTGTCACCTGCTCAACATCA-3′, 5′-TGGAATCTTCCGGCTGTAGGA-3′,and 5′-TexasRed-AGGTCTC- CACCACTGCCCTTGCTG-BHQ2-3′; IL-10,5′-TCGGAAATGATC- CAGTTTTACCTG-3′,5′-TCACAGGGGAGAAATCGATGAC-3′,and 5′-TexasRed-AGCCGCATCCTGAGGGTCTTCAGC-BHQ2-3′; G-CSF,5′-CGTTCCCCTGGTCACTGTCA-3′,5′-GGGTGACACAGCTTG- TAGGTG-3′,and 5′-FAM-CGCTCTGCCACCATCCCTGCCTCT-BHQ1-3′; PKA-Ca,5′-CTCCCACCCTCCAAACTGTC-3′,5′-GACAGGGT- CAGTTGGCTACC-3′, and 5′-FAM-ACCCTCCCCAAACACCCTCCT- CAC-BHQ1-3′; PKA-Cb;5′-GATGGAATGTCTTGTCAGCATGG-3′, 5′-TCGTCCAGGAGTCCTCACTG-3′, and 5′-TexasRed-AGGCGCTCT- GACTCACTGCTGCAT-BHQ2-3′; Creb1a,5′-CCCAGCACTTCCTACA- CAGCCT-3′,5′-ATTGCCCCTGGAGTTGTTATGG-3′;and the b-actin reference, 5′-TCCATGAAATAAGTGGTTACAGGA-3′,5′-CAGAAG-CAATGCTGTCACCTT-3′,and 5′-HEX-TCCCTCACCCTCCCAAAAGC- CACC-BHQ1-3′.

Nuclear translocation of p65

The complementary DNA (cDNA) encoding the GFP-p65 fusion protein wasexcisedasanNhe I-Bam HI fragment (from a plasmid provided by D. Baltimore's laboratory) and subcloned into the pIRES1-Neo plasmid (AfCS barcode M0084IR1NEOK). The GFP-p65-IRES1-Neo cassette was excisedbydigestionwithNheIand Hpa I andinsertedattheNheIand PshA I sites of the pL_UX vector (AfCS barcode M0085PLUX01A) to generate pL_Ubi-GFPp65-IRES-Neo

(AfCS barcode M0375UGP65NA). Lentivirus was generated from pL_Ubi-GFPp65-IRES-Neo and used to create a stable RAW cell line as previously described (72). The GFP-p65 RAW cell line was maintained according to AfCS protocol PP00000159. Cells were plated at a density of 5×10^5 cells in 35-mm glass-bottom microwell dishes coated with poly-D-lysine (Mat Tek) the day before trans- location experiments were performed. The cells were replenished with 1.8 ml of fresh media 30 min before stimulation. Cells were pretreated with either media alone or 8Br-cAMP for 5 min before stimulation with either LPS (100 ng/ml LPS + 250 pM LBP) or LPS and 8Br-cAMP (100 mM), re- spectively. Images weretakenevery 2min from10to60 min afterstim- ulation on a confocal microscope with a 63x oil lens. GFP was excited at 488 nm and emission spectra were collected over the range 505 to 550 nm. For analysis of protein translocation data, cell and nucleus outlines were identified and input manually into a custom-written computer program; the program then extrapolated feature shapes for all frames throughout the time course, and performed fluorescence intensity integrations. Frac- tion nuclear values were computed as quotients of nuclear fluorescence to total cellular fluorescence, computed after background subtraction.

Western blotting analysis

The amounts of total protein in RAW 264.7 cells were determined by a previously described Western blotting protocol (72). Cytosolic and nuclear fractions were generated with the NE-PER kit (Pierce, Thermo Fisher); cytosolic and particulate fractions were isolated with a kit from Biovision (#K267-50). The following antisera were used: anti-PKA-Ca (Cell Signaling Technology, #4782), anti-PKA-Cb (Santa Cruz Biotechnology, sc-904), anti-PKA RIa (Biogenesis, 0200-0356), anti-PKA RIIb (BD #610626), anti-IkBa (Santa Cruz Biotechnology, sc-371), anti-AKAP95 [provided by V. Coghlan (44)], anti-p105 Ab1 [#1140 (66) obtained from NCI repository], anti-p105 Ab2 (Santa Cruz Biotechnology, sc-114), anti- hnRNPL (Santa Cruz Biotechnology, sc-28726) and anti-Rho GDI (BD Biosciences, R26320). The abundance of phosphorylated proteins was as- sessed by AfCS protocols PP00000177 and PP00000181 with the following antisera: anti-pVASP (Cell Signaling Technology, #3111), anti- pp65 (Cell Signaling Technology, #3037), anti-pPKA consensus (Cell Signaling Technology, #9621), and anti-pp105 (Cell Signaling Technol- ogy, #4806).

Electrophoretic mobility shift assay

Nuclear extracts were isolated with the NE-PER kit (Pierce). An NF-κB consensus probe (73) was biotinylated by the Biotin 3′ End DNA-Labeling Kit (Pierce). Following the LightShift Chemiluminescent EMSA kit protocol (Pierce), 6 μg of nuclear extract was incubated with 40 fmol of labeled probe. Supershift reactions were performed with antibodies against p50 (Santa Cruz Biotechnology, SC-114X) or p65 (Santa Cruz Biotechnology, SC-109X).

Immunoprecipitations

Mammalian expression constructs were generated for murine AKAP95 and p105 with the Gateway system as previously described (74). HEK 293 cells were transfected with FLAG-AKAP95 and Myc-p105 with Lipofectamine 2000 (Invitrogen) following the manufacturer's protocol. Protein complexes were immunoprecipitated 48 hours after transfection from detergent-soluble cell lysates with a standard protocol (75). Cytosolic and nuclear fractions were generated from RAW 264.7 cells and BMDMs with the NE-PER kit (Pierce, Thermo Fisher). Immunoprecipitations were carried out with the two antisera against p105 described above and following standard procedures (75).

In vitro PKA assay

GST fusion proteins representing 25 amino acid sequences encompassing Ser^{940} of murine p105 or Ser^{157} of human VASP were expressed in pGEX-4T-1 (Promega) and purified. Control

proteins were generated in which these Ser residues were substituted with Ala. In vitro PKA phosphorylation reactions were performed with the Kinase-Glo assay (Promega) according to the manufacturer's protocol.

Site-directed mutagenesis of p105

An entry clone encoding murine p105 was generated as previously described (74), and Ser→Ala and Ser→Asp mutations were introduced at the codon corresponding to Ser^{940} with the QuikChange mutagenesis kit (Stratagene). Retroviral expression constructs were generated by LR recombination (Invitrogen) to a pFB-Neo-derived destination vector incorporating an N-terminal YFP fusion. RAW cell lines stably expressing YFP-tagged WT and mutant p105 proteins were generated by retroviral infection as previously described (27).

Supplementary Material

Refer to Web version on PubMed Central for supplementary material.

Acknowledgments

This work was supported by National Institute of General Medical Sciences Grant U54 GM062114. We thank L. Cheadle for excellent technical assistance and Alliance for Cellular Signaling colleagues for insight and advice. We are grateful to M. Covert and D. Baltimore for provision of the GFP-p65 construct, V. Coghlan for AKAP95 antisera, and W. Frankel and Y. Yang for the AKAP95GT mice.

REFERENCES AND NOTES

1. Akira S, Uematsu S, Takeuchi O. Pathogen recognition and innate immunity. Cell 2006;124:783–801. [PubMed: 16497588]
2. Beutler B, Jiang Z, Georgel P, Crozat K, Croker B, Rutschmann S, Du X, Hoebe K. Genetic analysis of host resistance: Toll-like receptor signaling and immunity at large. Annu. Rev. Immunol 2006;24:353–389. [PubMed: 16551253]
3. Creagh EM, O'Neill LA. TLRs, NLRs and RLRs: A trinity of pathogen sensors that co-operate in innate immunity. Trends Immunol 2006;27:352–357. [PubMed: 16807108]
4. Butchar JP, Parsa KV, Marsh CB, Tridandapani S. Negative regulators of toll-like receptor 4-mediated macrophage inflammatory response. Curr. Pharm. Des 2006;12:4143–4153. [PubMed: 17100617]
5. Shibolet O, Podolsky DK. TLRs in the Gut. IV. Negative regulation of Toll-like receptors and intestinal homeostasis: Addition by subtraction. Am. J. Physiol. Gastrointest. Liver Physiol 2007;292:G1469–G1473. [PubMed: 17554134]
6. Wang X, Liu Y. Regulation of innate immune response by MAP kinase phosphatase-1. Cell. Signal 2007;19:1372–1382. [PubMed: 17512700]
7. Taganov KD, Boldin MP, Baltimore D. MicroRNAs and immunity: Tiny players in a big field. Immunity 2007;26:133–137. [PubMed: 17307699]
8. Roy CR, Mocarski ES. Pathogen subversion of cell-intrinsic innate immunity. Nat. Immunol 2007;8:1179–1187. [PubMed: 17952043]
9. Baldari CT, Tonello F, Paccani SR, Montecucco C. Anthrax toxins: A paradigm of bacterial immune suppression. Trends Immunol 2006;27:434–440. [PubMed: 16861036]
10. Natarajan M, Lin KM, Hsueh RC, Sternweis PC, Ranganathan R. A global analysis of cross-talk in a mammalian cellular signalling network. Nat. Cell Biol 2006;8:571–580. [PubMed: 16699502]
11. Pradervand S, Maurya MR, Subramaniam S. Identification of signaling components required for the prediction of cytokine release in RAW 264.7 macrophages. Genome Biol 2006;7:R11. [PubMed: 16507166]
12. Bourne HR, Lichtenstein LM, Melmon KL, Henney CS, Weinstein Y, Shearer GM. Modulation of inflammation and immunity by cyclic AMP. Science 1974;184:19–28. [PubMed: 4131281]

13. Ollivier V, Parry GC, Cobb RR, de Prost D, Mackman N. Elevated cyclic AMP inhibits NF-κB-mediated transcription in human monocytic cells and endothelial cells. J. Biol. Chem 1996;271:20828–20835. [PubMed: 8702838]
14. Parry GC, Mackman N. Role of cyclic AMP response element-binding protein in cyclic AMP inhibition of NF-κB-mediated transcription. J. Immunol 1997;159:5450–5456. [PubMed: 9548485]
15. Farmer P, Pugin J. β-adrenergic agonists exert their "anti-inflammatory" effects in monocytic cells through the IκB/NF-κB pathway. Am. J. Physiol. Lung Cell. Mol. Physiol 2000;279:L675–L682. [PubMed: 11000127]
16. Delgado M, Ganea D. Vasoactive intestinal peptide and pituitary adenylate cyclase-activating polypeptide inhibit nuclear factor-κB-dependent gene activation at multiple levels in the human monocytic cell line THP-1. J. Biol. Chem 2001;276:369–380. [PubMed: 11029467]
17. Pozo D, Guerrero JM, Calvo JR. Vasoactive intestinal peptide and pituitary adenylate cyclase-activating polypeptide inhibit LPS-stimulated MIP-1α production and mRNA expression. Cytokine 2002;18:35–42. [PubMed: 12090758]
18. Vassiliou E, Jing H, Ganea D. Prostaglandin E2 inhibits TNF production in murine bone marrow-derived dendritic cells. Cell. Immunol 2003;223:120–132. [PubMed: 14527510]
19. Jing H, Yen JH, Ganea D. A novel signaling pathway mediates the inhibition of CCL3/4 expression by prostaglandin E2. J. Biol. Chem 2004;279:55176–55186. [PubMed: 15498767]
20. Aronoff DM, Canetti C, Serezani CH, Luo M, Peters-Golden M. Cutting edge: Macrophage inhibition by cyclic AMP (cAMP): Differential roles of protein kinase A and exchange protein directly activated by cAMP-1. J. Immunol 2005;174:595–599. [PubMed: 15634874]
21. Aronoff DM, Carstens JK, Chen GH, Toews GB, Peters-Golden M. Short communication: Differences between macrophages and dendritic cells in the cyclic AMP-dependent regulation of lipopolysaccharide-induced cytokine and chemokine synthesis. J. Interferon Cytokine Res 2006;26:827–833. [PubMed: 17115901]
22. Bryn T, Mahic M, Enserink JM, Schwede F, Aandahl EM, Taskén K. The cyclic AMP-Epac1-Rap1 pathway is dissociated from regulation of effector functions in monocytes but acquires immunoregulatory function in mature macrophages. J. Immunol 2006;176:7361–7370. [PubMed: 16751380]
23. Hata AN, Breyer RM. Pharmacology and signaling of prostaglandin receptors: Multiple roles in inflammation and immune modulation. Pharmacol. Ther 2004;103:147–166. [PubMed: 15369681]
24. Walsh DA, Perkins JP, Krebs EG. An adenosine 3′,5′-monophosphate-dependant protein kinase from rabbit skeletal muscle. J. Biol. Chem 1968;243:3763–3765. [PubMed: 4298072]
25. de Rooij J, Zwartkruis FJ, Verheijen MH, Cool RH, Nijman SM, Wittinghofer A, Bos JL. Epac is a Rap1 guanine-nucleotide-exchange factor directly activated by cyclic AMP. Nature 1998;396:474–477. [PubMed: 9853756]
26. Christensen AE, Selheim F, de Rooij J, Dremier S, Schwede F, Dao KK, Martinez A, Maenhaut C, Bos JL, Genieser HG, Døskeland SO. cAMP analog mapping of Epac1 and cAMP kinase. Discriminating analogs demonstrate that Epac and cAMP kinase act synergistically to promote PC-12 cell neurite extension. J. Biol. Chem 2003;278:35394–35402. [PubMed: 12819211]
27. Zhu X, Santat LA, Chang MS, Liu J, Zavzavadjian JR, Wall EA, Kivork C, Simon MI, Fraser ID. A versatile approach to multiple gene RNA interference using microRNA-based short hairpin RNAs. BMC Mol. Biol 2007;8:98. [PubMed: 17971228]
28. Zeng Y, Wagner EJ, Cullen BR. Both natural and designed micro RNAs can inhibit the expression of cognate mRNAs when expressed in human cells. Mol. Cell 2002;9:1327–1333. [PubMed: 12086629]
29. Butt E, Abel K, Krieger M, Palm D, Hoppe V, Hoppe J, Walter U. cAMP- and cGMP-dependent protein kinase phosphorylation sites of the focal adhesion vasodilator-stimulated phosphoprotein (VASP) in vitro and in intact human platelets. J. Biol. Chem 1994;269:14509–14517. [PubMed: 8182057]
30. Wong W, Scott JD. AKAP signalling complexes: Focal points in space and time. Nat. Rev. Mol. Cell Biol 2004;5:959–970. [PubMed: 15573134]
31. Jarnaess E, Taskén K. Spatiotemporal control of cAMP signalling processes by anchored signalling complexes. Biochem. Soc. Trans 2007;35:931–937. [PubMed: 17956249]

32. Carr DW, Hausken ZE, Fraser ID, Stofko-Hahn RE, Scott JD. Association of the type II cAMP-dependent protein kinase with a human thyroid RII-anchoring protein. Cloning and characterization of the RII-binding domain. J. Biol. Chem 1992;267:13376–13382. [PubMed: 1618839]
33. Huang LJ, Durick K, Weiner JA, Chun J, Taylor SS. Identification of a novel protein kinase A anchoring protein that binds both type I and type II regulatory subunits. J. Biol. Chem 1997;272:8057–8064. [PubMed: 9065479]
34. Carlson CR, Lygren B, Berge T, Hoshi N, Wong W, Taskén K, Scott JD. Deline-ation of type I protein kinase A-selective signaling events using an RI anchoring disruptor. J. Biol. Chem 2006;281:21535–21545. [PubMed: 16728392]
35. Karin M, Ben-Neriah Y. Phosphorylation meets ubiquitination: The control of NF-κB activity. Annu. Rev. Immunol 2000;18:621–663. [PubMed: 10837071]
36. Zhong H, SuYang H, Erdjument-Bromage H, Tempst P, Ghosh S. The transcriptional activity of NF-κB is regulated by the IκB-associated PKAc subunit through a cyclic AMP-independent mechanism. Cell 1997;89:413–424. [PubMed: 9150141]
37. Sakurai H, Chiba H, Miyoshi H, Sugita T, Toriumi W. IκB kinases phosphorylate NF-κB p65 subunit on serine 536 in the transactivation domain. J. Biol. Chem 1999;274:30353–30356. [PubMed: 10521409]
38. Zhong H, May MJ, Jimi E, Ghosh S. The phosphorylation status of nuclear NF-κB determines its association with CBP/p300 or HDAC-1. Mol. Cell 2002;9:625–636. [PubMed: 11931769]
39. Vermeulen L, De Wilde G, Van Damme P, Vanden Berghe W, Haegeman G. Transcriptional activation of the NF-κB p65 subunit by mitogen- and stress-activated protein kinase-1 (MSK1). EMBO J 2003;22:1313–1324. [PubMed: 12628924]
40. Caivano M, Gorgoni B, Cohen P, Poli V. The induction of cyclooxygenase-2 mRNA in macrophages is biphasic and requires both CCAAT enhancer-binding protein β (C/EBPβ) and C/EBPδ transcription factors. J. Biol. Chem 2001;276:48693–48701. [PubMed: 11668179]
41. Guan H, Hou S, Ricciardi RP. DNA binding of repressor nuclear factor-κB p50/p50 depends on phosphorylation of Ser337 by the protein kinase A catalytic subunit. J. Biol. Chem 2005;280:9957–9962. [PubMed: 15642694]
42. Meffert MK, Chang JM, Wiltgen BJ, Fanselow MS, Baltimore D. NF-κB functions in synaptic signaling and behavior. Nat. Neurosci 2003;6:1072–1078. [PubMed: 12947408]
43. Heissmeyer V, Krappmann D, Wulczyn FG, Scheidereit C. NF-κB p105 is a target of IκB kinases and controls signal induction of Bcl-3-p50 complexes. EMBO J 1999;18:4766–4778. [PubMed: 10469655]
44. Coghlan VM, Langeberg LK, Fernandez A, Lamb NJ, Scott JD. Cloning and characterization of AKAP 95, a nuclear protein that associates with the regulatory subunit of type II cAMP-dependent protein kinase. J. Biol. Chem 1994;269:7658–7665. [PubMed: 8125992]
45. Yang Y, Mahaffey CL, Bérubé N, Frankel WN. Interaction between fidgetin and protein kinase A-anchoring protein AKAP95 is critical for palatogenesis in the mouse. J. Biol. Chem 2006;281:22352–22359. [PubMed: 16751186]
46. Rouzer CA, Kingsley PJ, Wang H, Zhang H, Morrow JD, Dey SK, Marnett LJ. Cyclooxygenase-1-dependent prostaglandin synthesis modulates tumor necrosis factor-α secretion in lipopolysaccharide-challenged murine resident peritoneal macrophages. J. Biol. Chem 2004;279:34256–34268. [PubMed: 15181007]
47. Hayden MS, Ghosh S. Shared principles in NF-κB signaling. Cell 2008;132:344–362. [PubMed: 18267068]
48. Heissmeyer V, Krappmann D, Hatada EN, Scheidereit C. Shared pathways of IκB kinase-induced $SCF^{\beta TrCP}$-mediated ubiquitination and degradation for the NF-κB precursor p105 and IκBα. Mol. Cell. Biol 2001;21:1024–1035. [PubMed: 11158290]
49. Orian A, Gonen H, Bercovich B, Fajerman I, Eytan E, Israël A, Mercurio F, Iwai K, Schwartz AL, Ciechanover A. $SCF^{\beta\text{-}TrCP}$ ubiquitin ligase-mediated processing of NF-κB p105 requires phosphorylation of its C-terminus by IκB kinase. EMBO J 2000;19:2580–2591. [PubMed: 10835356]
50. Minami M, Shimizu K, Okamoto Y, Folco E, Ilasaca ML, Feinberg MW, Aikawa M, Libby P. Prostaglandin E receptor type 4-associated protein interacts directly with NF-κB1 and attenuates macrophage activation. J. Biol. Chem 2008;283:9692–9703. [PubMed: 18270204]

51. Platzer C, Meisel C, Vogt K, Platzer M, Volk HD. Up-regulation of monocytic IL-10 by tumor necrosis factor-α and cAMP elevating drugs. Int. Immunol 1995;7:517–523. [PubMed: 7547677]
52. Kitabayashi A, Hirokawa M, Hatano Y, Lee M, Kuroki J, Niitsu H, Miura AB. Granulocyte colony-stimulating factor downregulates allogeneic immune responses by posttranscriptional inhibition of tumor necrosis factor-α production. Blood 1995;86:2220–2227. [PubMed: 7545022]
53. Boneberg EM, Hartung T. Granulocyte colony-stimulating factor attenuates LPS-stimulated IL-1β release via suppressed processing of proIL-1β, whereas TNF-α release is inhibited on the level of pro TNF-α formation. Eur. J. Immunol 2002;32:1717–1725. [PubMed: 12115655]
54. Hareng L, Meergans T, von Aulock S, Volk HD, Hartung T. Cyclic AMP increases endogenous granulocyte colony-stimulating factor formation in monocytes and THP-1 macrophages despite attenuated TNF-α formation. Eur. J. Immunol 2003;33:2287–2296. [PubMed: 12884304]
55. Davies SP, Reddy H, Caivano M, Cohen P. Specificity and mechanism of action of some commonly used protein kinase inhibitors. Biochem. J 2000;351:95–105. [PubMed: 10998351]
56. Skålhegg BS, Huang Y, Su T, Idzerda RL, McKnight GS, Burton KA. Mutation of the Ca subunit of PKA leads to growth retardation and sperm dysfunction. Mol. Endocrinol 2002;16:630–639. [PubMed: 11875122]
57. Watanabe S, Kobayashi T, Okuyama H. Regulation of lipopolysaccharide-induced tumor necrosis factor a production by endogenous prostaglandin E2 in rat resident and thioglycollate-elicited macrophages. J. Lipid Mediat. Cell Signal 1994;10:283–294. [PubMed: 7812678]
58. Jin SL, Conti M. Induction of the cyclic nucleotide phosphodiesterase PDE4B is essential for LPS-activated TNF-α responses. Proc. Natl. Acad. Sci. U.S.A 2002;99:7628–7633. [PubMed: 12032334]
59. Bonner JC, Rice AB, Ingram JL, Moomaw CR, Nyska A, Bradbury A, Sessoms AR, Chulada PC, Morgan DL, Zeldin DC, Langenbach R. Susceptibility of cyclooxygenase-2-deficient mice to pulmonary fibrogenesis. Am. J. Pathol 2002;161:459–470. [PubMed: 12163371]
60. Wang JW, Howson J, Haller E, Kerr WG. Identification of a novel lipopolysaccharide-inducible gene with key features of both A kinase anchor proteins and chs1/beige proteins. J. Immunol 2001;166:4586–4595. [PubMed: 11254716]
61. Williams RO. Cutting edge: A-kinase anchor proteins are involved in maintaining resting T cells in an inactive state. J. Immunol 2002;168:5392–5396. [PubMed: 12023330]
62. Asirvatham AL, Galligan SG, Schillace RV, Davey MP, Vasta V, Beavo JA, Carr DW. A-kinase anchoring proteins interact with phosphodiesterases in T lymphocyte cell lines. J. Immunol 2004;173:4806–4814. [PubMed: 15470020]
63. Shibolet O, Giallourakis C, Rosenberg I, Mueller T, Xavier RJ, Podolsky DK. AKAP13, a RhoA GTPase-specific guanine exchange factor, is a novel regulator of TLR2 signaling. J. Biol. Chem 2007;282:35308–35317. [PubMed: 17878165]
64. Cinel I, Opal SM. Molecular biology of inflammation and sepsis: A primer. Crit. Care Med 2009;37:291–304. [PubMed: 19050640]
65. Kamada S, Kikkawa U, Tsujimoto Y, Hunter T. A-kinase-anchoring protein 95 functions as a potential carrier for the nuclear translocation of active caspase 3 through an enzyme-substrate-like association. Mol. Cell. Biol 2005;25:9469–9477. [PubMed: 16227597]
66. Rice NR, MacKichan ML, Israël A. The precursor of NF-kBp50hasIkB-like functions. Cell 1992;71:243–253. [PubMed: 1423592]
67. Baeuerle PA, Baltimore D. IkB: A specific inhibitor of the NF-kB transcription factor. Science 1988;242:540–546. [PubMed: 3140380]
68. Basak S, Kim H, Kearns JD, Tergaonkar V, O'Dea E, Werner SL, Benedict CA, Ware CF, Ghosh G, Verma IM, Hoffmann A. A fourth IkB protein within the NF-kB signaling module. Cell 2007;128:369–381. [PubMed: 17254973]
69. Mata-Haro V, Cekic C, Martin M, Chilton PM, Casella CR, Mitchell TC. The vaccine adjuvant monophosphoryl lipid A as a TRIF-biased agonist of TLR4. Science 2007;316:1628–1632. [PubMed: 17569868]
70. Pawson T. Dynamic control of signaling by modular adaptor proteins. Curr. Opin. Cell Biol 2007;19:112–116. [PubMed: 17317137]
71. Shin KJ, Wall EA, Zavzavadjian JR, Santat LA, Liu J, Hwang JI, Rebres R, Roach T, Seaman W, Simon MI, Fraser ID. A single lentiviral vector platform for microRNA-based conditional RNA

interference and coordinated transgene expres- sion. Proc. Natl. Acad. Sci. U.S.A 2006;103:13759–13764. [PubMed: 16945906]

72. Fraser I, Liu W, Rebres R, Roach T, Zavzavadjian J, Santat L, Liu J, Wall E, Mumby M. The use of RNA interference to analyze protein phosphatase function in mammalian cells. Methods Mol. Biol 2007;365:261–286. [PubMed: 17200568]
73. Hou S, Guan H, Ricciardi RP. Phosphorylation of serine 337 of NF-kB p50 is critical for DNA binding. J. Biol. Chem 2003;278:45994–45998. [PubMed: 12947093]
74. Zavzavadjian JR, Couture S, Park WS, Whalen J, Lyon S, Lee G, Fung E, Mi Q, Liu J, Wall E, Santat L, Dhandapani K, Kivork C, Driver A, Zhu X, Chang MS, Randhawa B, Gehrig E, Bryan H, Verghese M, Maer A, Saunders B, Ning Y, Subramaniam S, Meyer T, Simon MI, O'Rourke N, Chandy G, Fraser ID. The alliance for cellular signaling plasmid collection: A flexible resource for protein localization studies and signaling pathway analysis. Mol. Cell. Proteomics 2007;6:413–424. [PubMed: 17192258]
75. Fraser ID, Tavalin SJ, Lester LB, Langeberg LK, Westphal AM, Dean RA, Marrion NV, Scott JD. A novel lipid-anchored A-kinase Anchoring Protein facilitates cAMP-responsive membrane events. EMBO J 1998;17:2261–2272. [PubMed: 9545239]

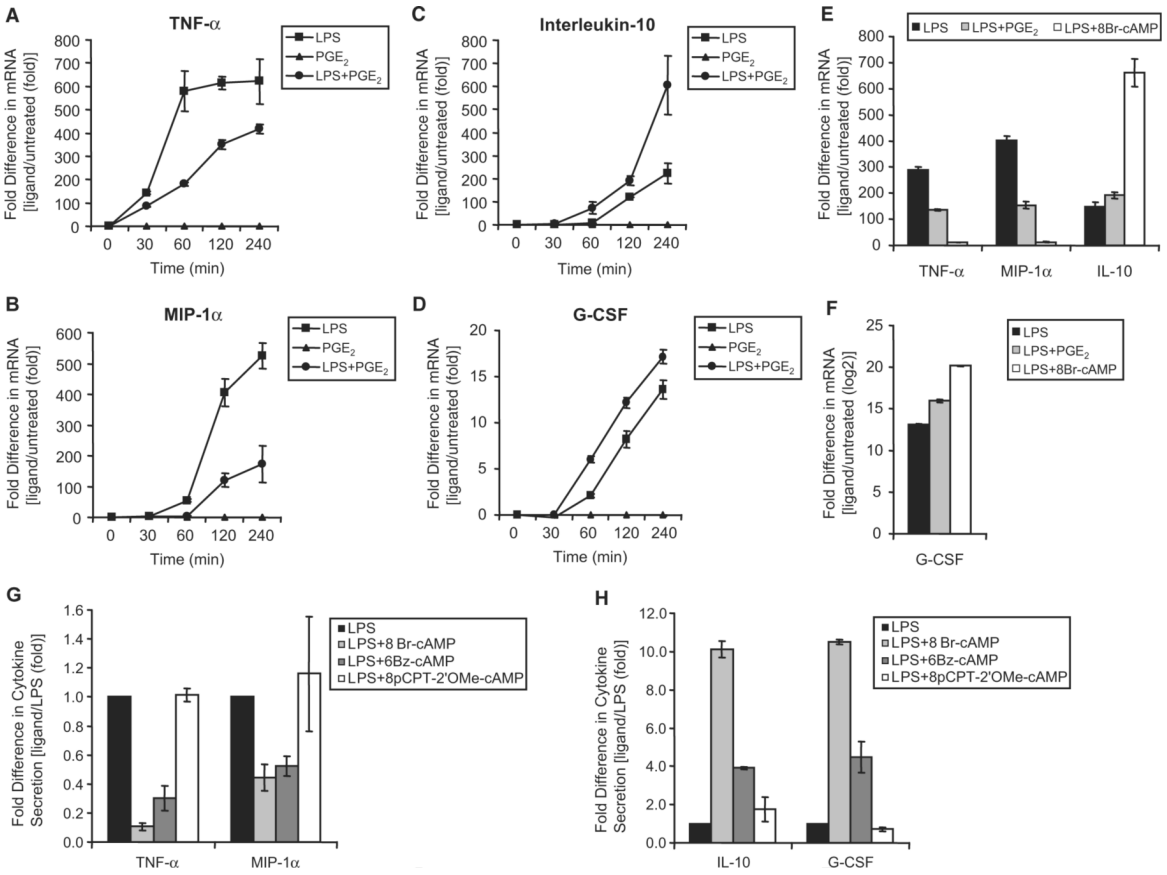

Fig. 1.

PGE_2 modulates LPS-induced expression of cytokines in RAW cells through a cAMP-dependent pathway. (**A** to **D**) RAW 264.7 cells were stimulated for up to 4 hours with LPS [LPS (100 ng/ml) + 250 pM LBP], PGE_2 (10 μM), or both ligands. The abundances of mRNAs of *TNF*-α (A), *MIP-1*α (B), *IL-10* (C), and *G-CSF* (D) were assessed by quantitative, real-time RT-PCR and compared to those in untreated RAW 264.7 cells. (**E** and **F**) RAW cells were stimulated for 2 hours with LPS [LPS (100 ng/ml) + 250 pM LBP], LPS and PGE_2 (10 μM), or LPS and 8Br-cAMP (100 μM), and the abundance of mRNAs in these cells compared to that in untreated RAW 264.7 cells were determined for *TNF*-α, *MIP-1*α, and *IL-10* (E) and *G-CSF* (F). Data represent the means ± SEM from at least four independent experiments carried out on separate days. (**G** and **H**) RAW 264.7 cells were stimulated for 4 hours with LPS (100 ng/ml), LPS and 8Br-cAMP (250 μM), LPS and 6Bz-cAMP (250 μM), or LPS and 8pCPT-2′ OMe-cAMP (250 μM) and the abundances of secreted TNF-α and MIP-1α (G) and IL-10 and G-CSF (H) were determined. Data represent the means ± SEM from at least two independent experiments carried out on separate days and are shown as the fold change in the abundance of each cytokine under each condition relative to that of LPS-treated cells.

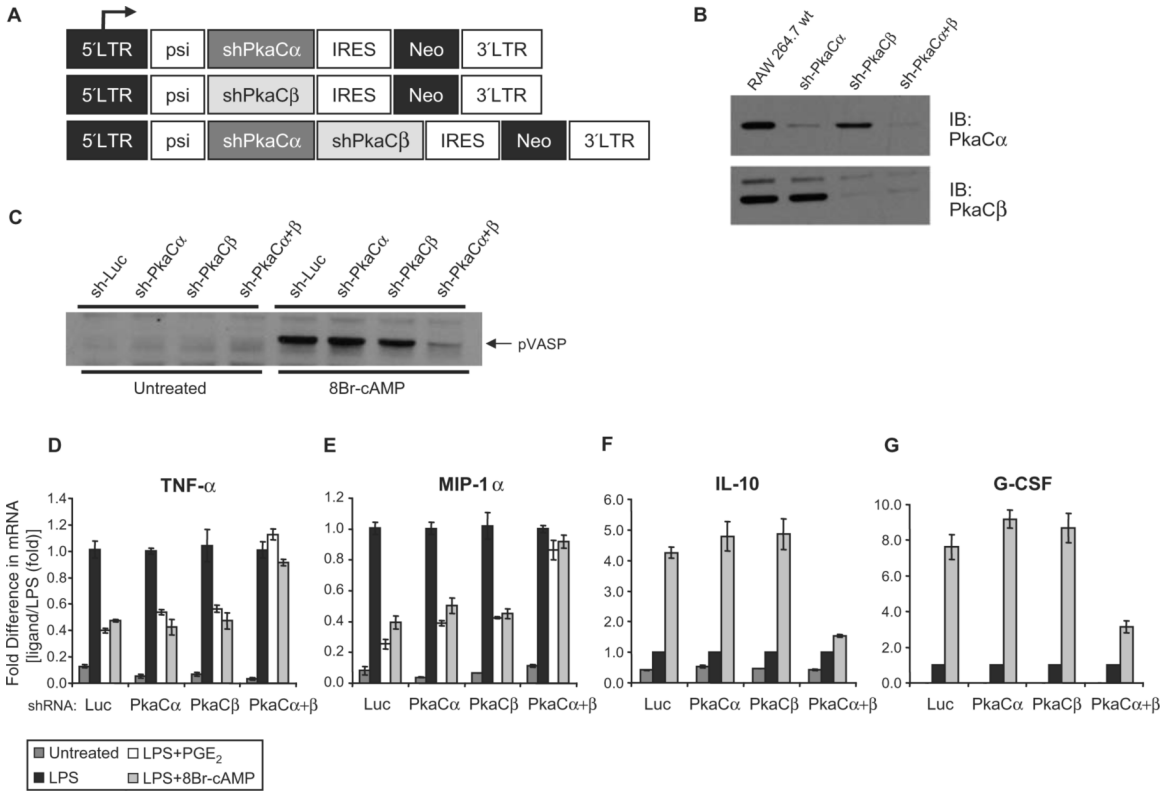

Fig. 2.

Multigene RNAi against both the α and the β catalytic subunits of PKA in RAW 264.7 cells is necessary to attenuate PKA-dependent phosphorylation and reverse cAMP-dependent modulation of the LPS-induced expression of cytokine genes. (**A**) Schematic of retroviral vectors that encode miR-shRNA designed to knockdown expression of PKA-Cα, PKA-Cβ, or both subunits. (**B**) Western blotting assessment of the abundance of PKA-Cα and PKA-Cβ mRNA and protein in stable RAW 264.7 cell lines expressing shRNA against either or both catalytic subunits. (**C**) Western blotting analysis with a phosphospecific antibody against Ser^{157} of VASP in PKA-C-specific miR-shRNA-expressing RAW cell lines. The abundance of phosphorylated VASP (pVASP) in both untreated cells and in cells stimulated with 8Br-cAMP (100 μM) for 30 min are shown. RAW 264.7 cell lines transfected with a control miR-shRNA (shLuc) vector or with miR-shRNA vectors specific for PKA-Cα (shPkaCα), PKA-Cβ (shPkaCβ), or both (shPkaCα+Cβ) were stimulated with LPS (100 ng/ml + 250 pM LBP), LPS and PGE_2 (10 μM) or LPS and 8Br-cAMP (100 μM) for 2 hours. The abundance of mRNAs for *TNF*-α (**D**), *MIP-1α* (**E**), *IL-10* (**F**), and *G-CSF* (**G**) in the treated cells were assessed by qPCR and are shown as the fold change in abundance relative to that of LPS-treated cells. Data from qPCR experiments are the means ± SEM from three samples taken 2 to 6 weeks after infection of cells with the given retroviruses. Western blots are representative of protein samples taken 4 to 8 weeks after the establishment of miR-shRNA-expressing RAW cell lines.

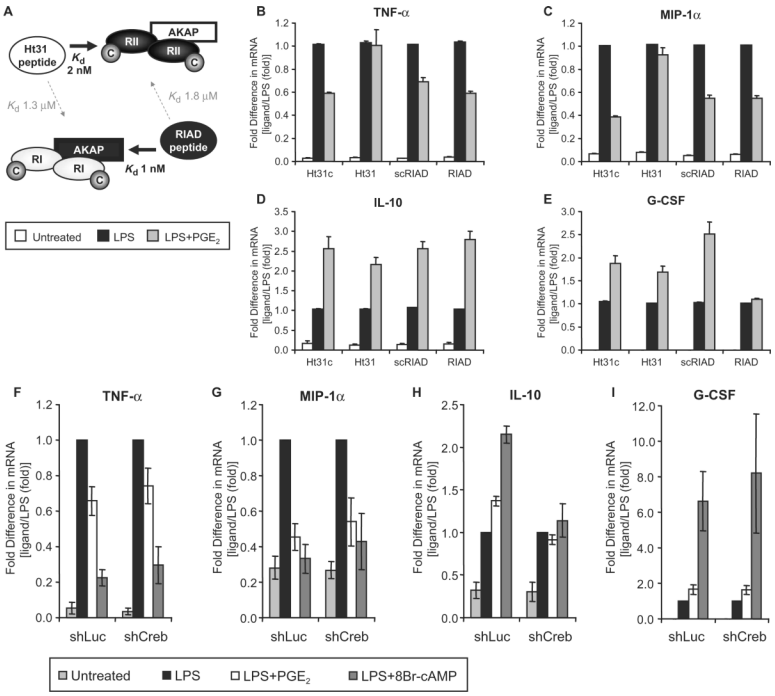

Fig. 3.

PKA-anchoring inhibitor peptides and depletion of CREB have differential effects on the cAMP-dependent modulation of LPS-induced expression of cytokine genes. (**A**) Schematic describing the selectivity of PKA-anchoring inhibitor peptides that preferentially disrupt either AKAP-RII complexes (Ht31) or AKAP-RI complexes (RIAD). RAW cells were pretreated for 30 min with 100 μM Ht31 or 50 μM RIAD (or with their respective control peptides Ht31c and scRIAD) and were then stimulated with LPS (100 ng/ml + 250 pM LBP) or LPS and PGE_2 (10 μM) for 2 hours. The abundances of mRNAs for *TNF*-α (**B**), *MIP-1α* (**C**), *IL-10* (**D**), and *G-CSF* (**E**) were determined by qPCR and are shown as the fold change in mRNA abundance in each sample relative to that of LPS-treated cells. RAW cell lines stably transfected with a control miR-shRNA (Luc) or miR-shRNA specific for Creb1a (shCreb) were generated. Each cell line was stimulated with LPS (100 ng/ml + 250 pM LBP), LPS and PGE_2 (10 μM), or LPS and 8Br-cAMP (100 μM) for 2 hours. The abundance of mRNAs for *TNF*-α (**F**), *MIP-1α* (**G**), *IL-10* (**H**), and *G-CSF* (**I**) were determined by qPCR and are shown as the fold change in mRNA abundance in each sample relative to that of LPS-treated cells. Data shown are the means ± SEM from at least four independent experiments. Analysis of the CREB-specific miR-shRNA-expressing RAW 264.7 cell lines was performed between 3 and 6 weeks after infection.

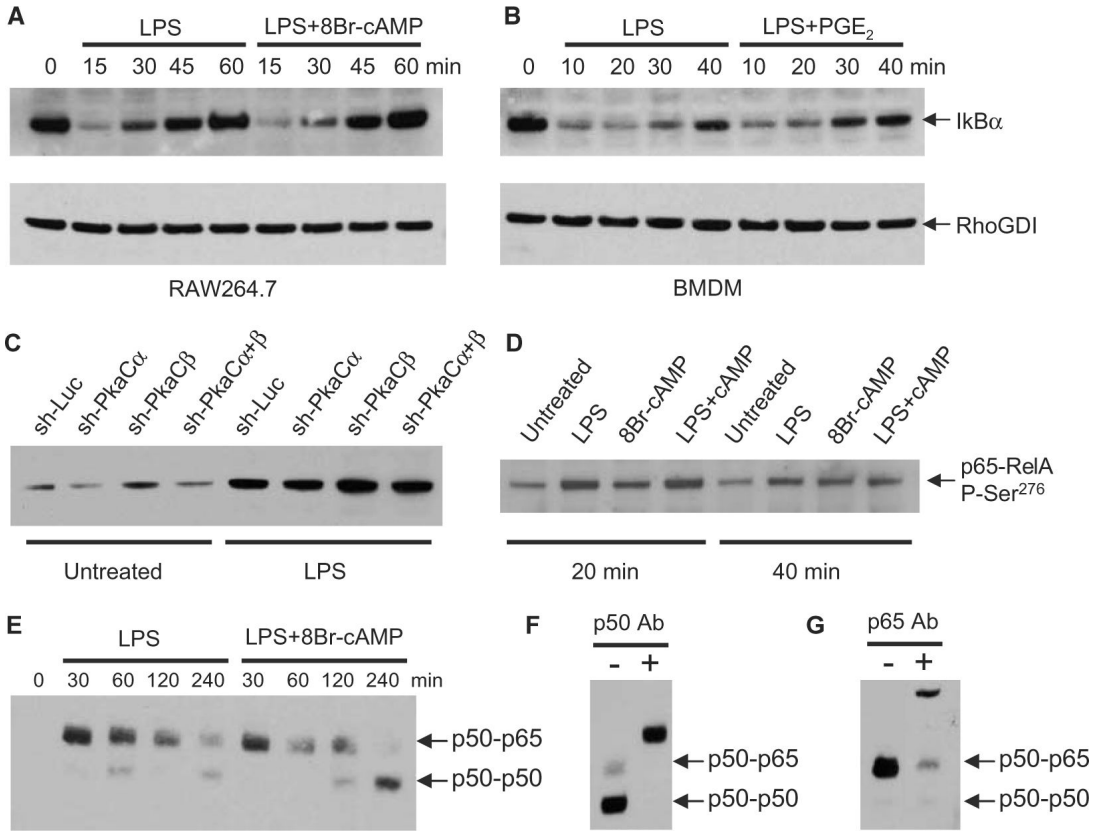

Fig. 4.

Analysis of the effects of cAMP and PKA on LPS-induced degradation of IκBα, phosphorylation of p65, and activation of NF-κB activation in macrophages. (**A**) Assessment of the abundance of cytoplasmic IκBα after stimulation of RAW 264.7 cells with either LPS (100 ng/ml + 250 pM LBP) or LPS and 8Br-cAMP (100 μM) for the indicated times. The abundance of RhoGDI in each sample is shown as a loading control. (**B**) Assessment of the abundance of cytoplasmic IκBα protein after stimulation of BMDMs with either LPS (100 ng/ml + 250 pM LBP) or LPS and PGE_2 (10 μM) for the indicated times. The abundance of RhoGDI in each sample is shown as a loading control. (**C**) Phosphorylation of p65 at Ser^{276} by 30 min of treatment with LPS in RAW 264.7 cells depleted of catalytic subunits of PKA. Knockdown of PKA-C subunits had no substantial effect on LPS-induced phosphorylation. (**D**) Phosphorylation of p65 at Ser^{276} in WT RAW 264.7 cells in response to either LPS, 8Br-cAMP, or LPS and 8Br-cAMP. (**E**) EMSAs showing the nuclear activation of NF-κB complexes in RAW 264.7 cells stimulated with either LPS (100 ng/ml + 250 pM LBP) or LPS and 8Br-cAMP (100 μM) for the indicated times. Nuclear accumulation of the p50–p65 heterodimer was attenuated by cAMP, whereas later accumulation of the p50–p50 homodimer was enhanced by cAMP. (**F**) Control EMSAs showing the supershift of p50–p50 and p50–p65 complexes (after 240 min of stimulation with LPS and 8Br-cAMP) in the presence of an antibody against p50. (**G**) Control EMSAs showing the supershift of only the p50–p65 complex (after 30 min of stimulation with LPS) in the presence of an antibody against p65. Data shown are representative of at least three independent experiments.

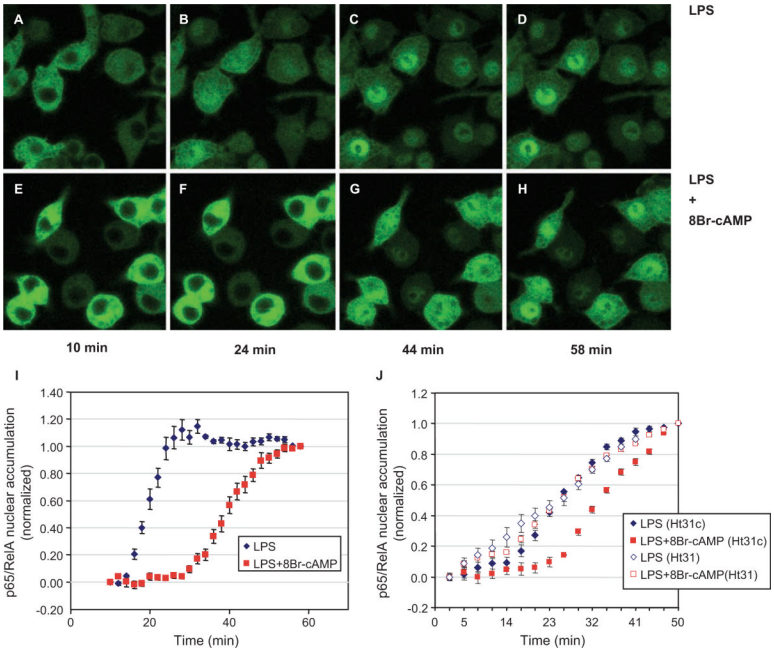

Fig. 5.

Analysis of the effects of cAMP and PKA on the LPS-induced translocation of p65 in RAW 264.7 cells. (**A** to **H**) Time-lapse confocal microscopy of RAW 264.7 cells stably expressing GFP-tagged p65. Stimulation of cells with LPS (A to D) induced substantial cytosolic-to-nuclear translocation of p65 by 24 min. Stimulation of cells with LPS in the presence of 8Br-cAMP (E to H) resulted in a substantial delay in the nuclear translocation of p65. (**I**) Collated data from the experiments represented in (A) to (H) derived from multiple single cells ($n = 9$). Nuclear accumulation of p65 was determined by measuring the relative fluorescent intensity in the nucleus before stimulation (=0) and after stimulation (=1). (**J**) The effect of cAMP on the LPS-induced nuclear accumulation of p65 in the presence of either control peptide (Ht31c) or the Ht31 inhibitor peptide. The cAMP-dependent attenuation in the nuclear accumulation of p65 was lost in the presence of Ht31. Data shown are representative of at least two independent experiments.

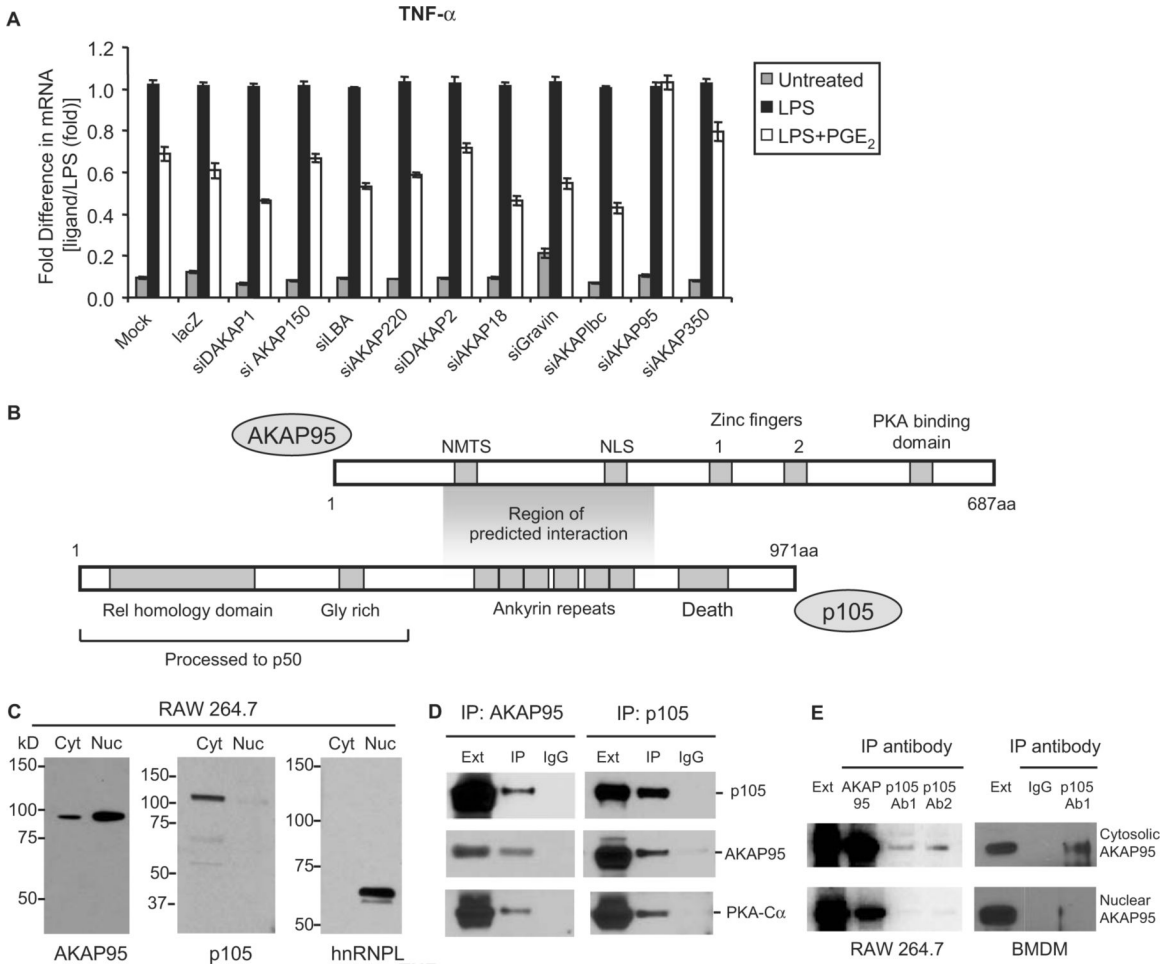

Fig. 6.

AKAP95 is required for PGE_2-dependent attenuation of LPS-induced expression of *TNF*-α and forms a cytoplasmic complex with p105. (**A**) RAW 264.7 cells were transfected with the indicated siRNAs; 72 hours after transfection, cells were stimulated with LPS (100 ng/ml + 250 pM LBP) or LPS + PGE_2 (10 μM) for 1 hour and the adundance of *TNF*-α mRNA in each sample was assessed by qPCR. (**B**) A schematic diagram showing the domain structure and predicted regions of interaction between AKAP95 and p105. NMTS, nuclear membrane-targeting sequence; NLS, nuclear localization sequence. (**C**) Assessment of AKAP95, p105, and hnRNPL (included as a nuclear positive control) in cytosolic (Cyt) and nuclear (Nuc) fractions of RAW 264.7 cells. (**D**) Either FLAG-AKAP95 or Myc-p105 was immunoprecipitated (IP) from detergent-soluble HEK 293 cell lysates and analyzed by Western blotting for the presence of AKAP95, p105, and PKA-Cα.(**E**) Cytosolic and nuclear fractions were isolated from RAW 264.7 cells and BMDMs and subjected to immunoprecipitation with either control antisera [immunoglobulin G (IgG)] or antisera against p105 (Ab1 or Ab2, see Materials and Methods). AKAP95 was detected by Western blotting. qPCR data shown are the means ± SEM from four independent transfections. Western blots are representative of at least two experiments.

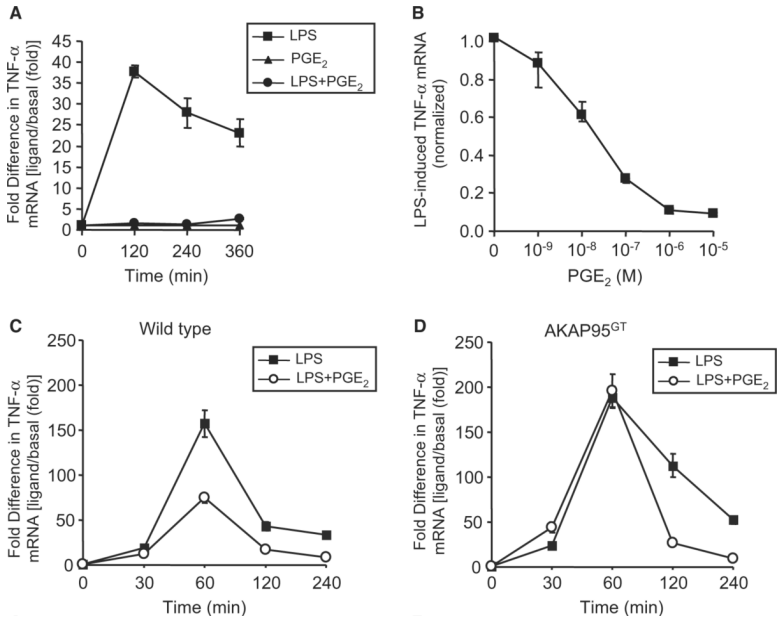

Fig. 7.

PGE_2 attenuates LPS-induced expression of *TNF*-α in BMDMs and the early stage of attenuation is lost in BMDMs from $AKAP95^{GT}$ mice. (**A**) BMDMswere stimulated for up to 6 hours with LPS (100 ng/ml + 250 pM LBP), PGE_2 (10 μM), or both ligands, and the abundance of *TNF*-α mRNA in each sample was assessed by qPCR. (**B**) BMDMs were stimulated for 2 hours with LPS (100 ng/ml + 250 pM LBP) and increasing concentrations of PGE_2, and the abundance of *TNF*-α mRNA in each sample was assessed by qPCR. BMDMs derived from either WT mice (**C**) or $AKAP95^{GT}$ mice (**D**) were stimulated for up to 4 hours with LPS (100 ng/ml + 250 pM LBP) or LPS and PGE_2 (50 nM), and the abundance of *TNF*-α mRNA in each sample was assessed by qPCR. Data shown represent the means ± SEM from at least four independent experiments and from three nonlittermate $AKAP95^{GT}$ mice.

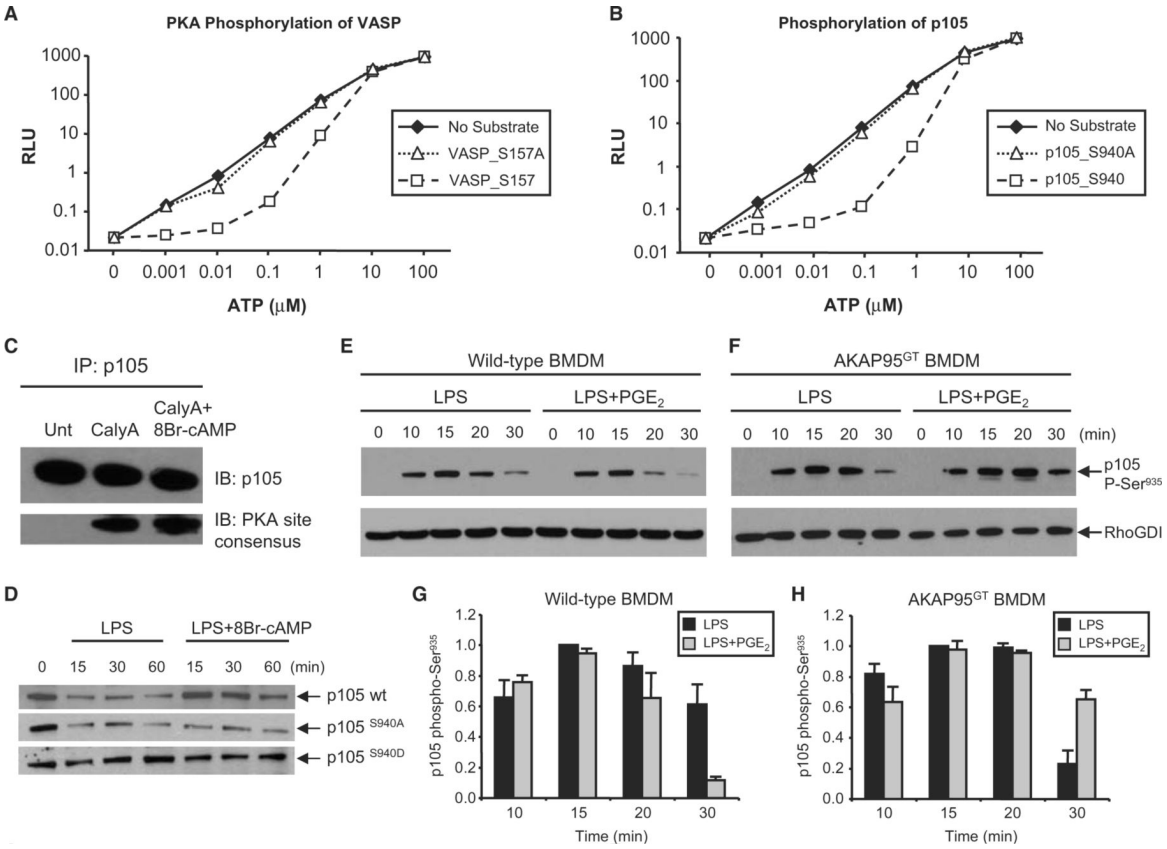

Fig. 8.

Phosphorylation of p105 at Ser^{940} by PKA and its influence on the phosphorylation of IKK and the degradation of p105. In vitro PKA-mediated phosphorylation of GST fusion proteins containing either a known PKA phosphorylation site in VASP (Ser^{157}) or a predicted PKA phosphorylation site in p105 (Ser^{940}). Phosphorylation by purified PKA-C subunit was indicated by the reduction in ATP-dependent luciferase activity because of kinase-dependent depletion of ATP. Phosphorylation was observed for both VASP Ser^{157} (**A**) and p105 Ser^{940} (**B**), but not with control proteins containing Ser→Ala substitutions. RLU, relative light unit. (**C**) Western blotting analysis of p105 immunoprecipitated from RAW cells treated with calyculin A (CalyA) or calyculin A and 8Br-cAMP. Comparable amounts of p105 protein were recovered from all samples, but a 105-kD band was detected with an antibody to phospho PKA only in the treated cells. (**D**) The abundance of WT and mutant p105 proteins after treatment of RAW cell lines expressing a yellow fluorescent protein (YFP)-tagged p105 protein with either LPS (100 ng/ml + 250 pM LBP) or LPS and 8Br-cAMP (100 μM) for the indicated times. Assessment of the phosphorylation of p105 by IKK at Ser^{935} after stimulation of BMDMs derived from WT mice (**E**) or $AKAP95^{GT}$ mice (**F**) with either LPS (100 ng/ml + 250 pM LBP) or LPS and PGE_2 (50 nM) for the indicated times. The abundance of RhoGDI in each sample is shown as a loading control. The average amounts of p105 proteins phosphorylated at Ser^{935} from triplicate experiments were quantified for BMDMs derived from WT mice (**G**) and $AKAP95^{GT}$ mice (**H**). All data are representative of at least three independent experiments.

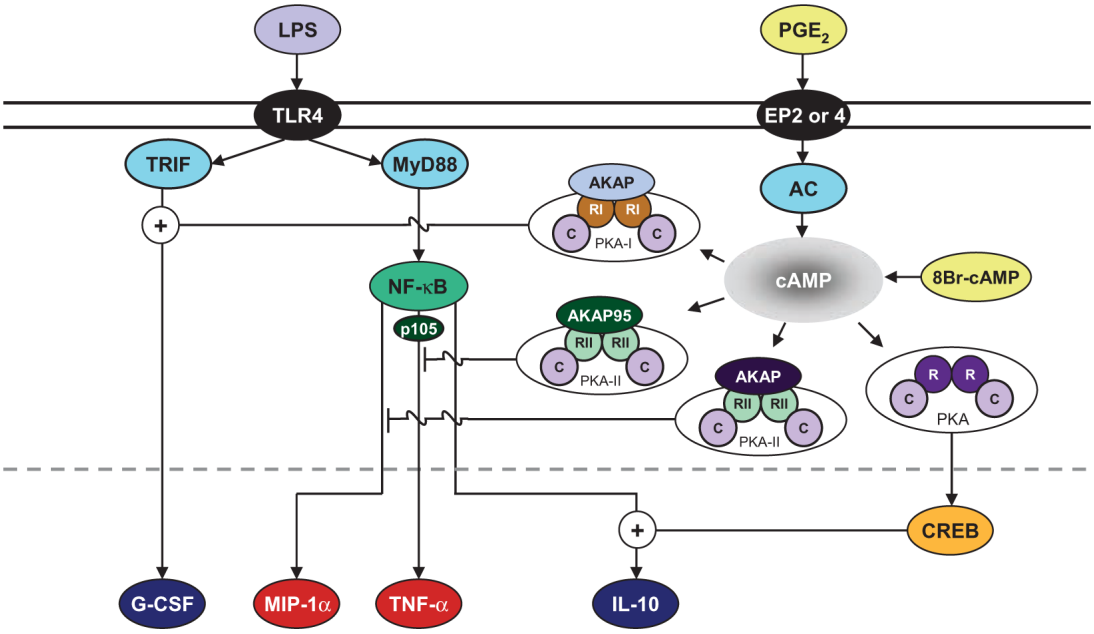

Fig. 9.

A proposed schematic for the mechanisms through which PKA may modulate LPS-induced expression of cytokine genes in macrophages. LPS induces the expression of genes encoding both proinflammatory (TNF-α, MIP-1α) and anti-inflammatory (IL-10, G-CSF) cytokines. cAMP promotes an anti-inflammatory cytokine profile through suppression of LPS-induced expression of *TNF*-α and *MIP-1α* and enhancement of LPS-induced expression of *IL-10* and *G-CSF*. These effects of cAMP are achieved in part through scaffolding interactions that localize type I PKA (PKA-I) to enhance expression of *G-CSF* and type II PKA (PKA-II) to inhibit NF-κB-induced expression of *TNF*-α and *MIP-1α*. Suppression of the expression of *TNF*-α involves the targeting of type-II PKA by AKAP95 to an NF-κB complex that includes p105. The PKA-dependent enhancement of LPS-induced expression of *IL-10* occurs through a scaffolding-independent mechanism that requires CREB.